# Impacts of spatiotemporal index standardization on the stock assessment of Norton Sound red king crab

Caitlin A. Stern
Alaska Department of Fish and Game
caitlin.stern@alaska.gov

September 2025

## Abstract

Indices of abundance are key inputs to stock assessment models, influencing model outputs that shape fisheries management decisions. Design-based methods for producing these indices from fishery-independent surveys come with potential drawbacks, including highly variable estimates when spatial dependence in survey catch is present yet excluded from calculations, and biased results when survey sampling deviates from survey design. Implications for stock assessment models include the potential for better predictive ability when using model-based rather than design-based indices. The stock assessment for red king crab (*Paralithodes camtschaticus*) in Norton Sound, Alaska, uses design-based indices of abundance based on three fishery-independent surveys. These surveys cover different years and areas, and within a survey the locations sampled sometimes varies among years, suggesting a need for spatiotemporal standardization to improve abundance estimation. Here, I evaluate the effects on key outputs of the stock assessment model of using design-based survey indices versus a spatiotemporally standardized model-based index of abundance. Fits to size composition data were similar for models using design-based versus model-based indices, while fits to standardized fishery catch per unit effort indices were poorer for models using model-based indices. Retrospective patterns were less extreme for models using the spatiotemporal model-based index, indicating an improved ability to predict stock biomass in the terminal year. The estimated scale of the population was lower across the time series when using the model-based index. While estimated stock status was comparable or higher when using the spatiotemporal model-based index, model-estimated abundance was reduced, as was recommended harvest.

## Introduction

Indices of abundance are key inputs to stock assessment models, providing information crucial for estimating stock size (Patterson et al. 2001; Maunder and Punt 2004). However, design-based methods for producing these indices from fishery-independent surveys can yield biased results when practical constraints lead survey sampling to deviate from survey design. For example, financial resources may not be sufficient for surveys to occur as frequently as planned, or weather conditions may limit vessels to sampling only a subset of survey stations. Spatiotemporal models including spatial and spatiotemporal random effects have the potential to mitigate the effects of inconsistent survey sampling by accounting for the spatiotemporal processes that underlie survey observations (Thorson et al. 2021; Yalcin et al. 2023). Simulation work suggests than index standardization using well-specified spatiotemporal models can reduce the impact of changes in survey effort by providing a consistent method of inferring abundance in missing areas (Yalcin et al. 2023).

In addition to suffering from bias due to changes in survey sampling, design-based indices of abundance can inflate temporal variability by failing to account for spatial dependence (Shelton et al. 2014; Thorson

et al. 2015). Due to the importance of indices of abundance in stock assessment models, this can lead to increased uncertainty in stock assessment model outputs used in fishery management (Cao et al. 2017). By accounting for spatial variation in survey catch, as well as incorporating habitat variables, spatiotemporal model-based index standardization can produce abundance indices with reduced variability compared to design-based indices (Cao et al. 2017, Chen et al. 2024). Important outcomes for stock assessment models can include less extreme retrospective patterns when using model-based rather than design-based indices (Cao et al. 2017, Chen et al. 2024).

The population of red king crab (*Paralithodes camtschaticus*) in Norton Sound, Alaska, supports locally important commercial and subsistence fisheries. The stock assessment for Norton Sound red king crab uses three fishery-independent trawl survey time series in design-based indices of abundance: the National Oceanic and Atmospheric Administration (NOAA) Norton Sound trawl survey (1976-1991), the Alaska Department of Fish and Game (ADF&G) trawl survey (1996-2024), and the NOAA Northern Bering Sea (NBS) trawl survey (2010-2023) (Stern and Palof 2025; Hamazaki 2024). The data sets from these surveys, all of which use a systematic sampling design, cover different years and spatial footprints, and within a survey the set of locations sampled sometimes varies among years (Figure 1). While the NOAA NBS trawl survey sampling has been consistent, with 35 stations sampled in 4 of 6 years and 34 stations sampled in the remaining two years, the number of stations sampled per year ranges from 53 to 104 for the NOAA NS trawl survey and 39 to 73 for the ADF&G trawl survey. This history of variation in survey sampling is one of the factors motivating the development of spatiotemporal model-based indices for this stock, as standardization over both space and time is required.

Initial work on a model-based approach for deriving Norton Sound red king crab survey indices of abundance led to the development of three separate model-based indices of abundance, one for each of the survey time series (Stern 2025). However, replacing the design-based indices of abundance with these model-based indices of abundance in the stock assessment model did not seem to improve key aspects of the stock assessment model, including the retrospective pattern (Stern and Palof 2025). Combining data from the three survey time series into a single model-based index of abundance has been a long-standing goal for this stock assessment, and seemed the logical next step given the lack of improvement following the incorporation of separate model-based indices. Here, I develop a single spatiotemporal model-based index of abundance for Norton Sound red king crab, and examine the effects on key model outputs of using this index in the stock assessment model.

# Methods

## Data sources

Following the Norton Sound red king crab stock assessment, I included data from the NOAA Norton Sound trawl survey (1976-1991), ADF&G trawl survey (1996-2024), and NOAA NBS trawl survey (2010-2023) on males with carapace length $\geq$ 64 mm. Initial model runs with data from all three surveys did not converge, probably due to lack of temporal overlap between the NOAA Norton Sound trawl survey time series and the other two survey time series. NOAA Norton Sound trawl survey data were excluded from subsequent spatiotemporal models, which focused on combining only data from the two survey time series that overlap in time.

Estimated density in crab/km$^2$ by survey station for each year of each survey is shown in Figures 2 - 4. The number of survey stations sampled per year ranged from 53 to 104 (median = 78.5) for the NOAA Norton Sound survey, 39 to 100 (median = 54.5) for the ADF&G trawl survey, and 34 to 35 (median = 35) for the NOAA NBS trawl survey. The modeled response variable, crab per km$^2$, is positive continuous with many zeros for each of the survey time series (Figure 5). The percentage of sampled stations that recorded zero males with carapace length $\geq$ 64 mm over all years in the time series was 48% for the NOAA Norton Sound trawl survey, 52% for the ADF&G trawl survey, and 59% for the NOAA NBS trawl survey.

## Spatiotemporal models

I fit geostatistical GLMMs with spatiotemporally correlated random effects to survey data using the R (R Core Team 2024) package **sdmTMB** (Anderson et al. 2022). In this approach, spatial effects are modeled using the stochastic partial differential equation (SPDE) approximation to Gaussian random fields (Lindgren et al. 2011). The rate at which spatial covariance decays with distance is defined by the Matèrn covariance function, a derived parameter of which is the spatial (or Matèrn) range, the distance at which spatial correlation decays such that two points are effectively independent (Anderson et al. 2022). While past attempts at spatiotemporal index standardization for Norton Sound red king crab used VAST, the authors of that work found VAST difficult to use (Hamazaki and Zheng 2021). I chose to use **sdmTMB** because, compared to VAST, **sdmTMB** has a simpler user interface and faster estimation times. **sdmTMB** uses geostatistical time series data to estimate spatial and spatiotemporal generalized linear mixed effects models (GLMMs). This approach allows for index standardization when the set of stations surveyed is not consistent across years: one can generate a spatial grid that covers the area of interest, predict from the model onto that grid, and sum the predicted abundance to obtain an area-weighted index that is independent of sampling locations (Anderson et al. 2022).

Applying the SPDE approach to modeling random fields requires defining a triangulation mesh of the spatial domain (Anderson et al. 2022). I constructed a triangulation mesh for each data set using the **sdmTMB** function make_mesh(), a wrapper for the triangulation mesh functions in the **fmesher** package (Lindgren 2023), and the **sdmTMBextra** (Anderson 2025) function add_barrier_mesh(). The add_barrier_mesh function permitted incorporation of correlation barriers based on the Norton Sound coastline. I specified a cut-off value of 20 for the minimum allowed distance between mesh vertices, which resulted in a mesh with 114 vertices for the data set without depth information and 93 vertices for the data set with depth information (Figures 6 and 7).

For all models, I estimated spatiotemporal random fields as independent and identically distributed (IID). The spatial random fields are estimated for each time slice, the period of which is specified in the model (e.g., time = year). Estimating spatiotemporal random fields as IID is likely most appropriate for the standardization of survey indices intended to be used in stock assessment models as this approach minimizes the estimation covariance among years, which is usually ignored in stock assessment models (Thorson et al. 2020, Chen et al. 2024). I compared models in which the fixed effects were year and survey identity (ADF&G or NOAA NBS), both specified as factors, with models that also included survey station depth (m; centered and scaled by its standard deviation) as a covariate, as variation in the depth of stations surveyed from year to year could influence estimated abundance if not taken into account. Minimum and maximum depth surveyed were relatively invariant for the NOAA NBS trawl survey, ranging from 11 to 12 m and 34 to 37 m across years in the time series, respectively. For the ADF&G trawl survey, minimum and maximum depth ranges across years in the time series were 3.29 - 13.2 m and 28.2 - 33.2 m, respectively.

## Model evaluation and diagnostics

After fitting models, I checked model convergence using the **sdmTMB** sanity() function. Models were considered converged if they met the following criteria evaluated by the sanity() function: the non-linear minimizer suggested successful convergence; the Hessian matrix was positive definite; no extreme or very small eigenvalues were detected; all gradients with respect to fixed effects were $< 0.001$; no fixed-effect standard errors were NA; no standard errors looked unreasonably large; no sigma parameters were $< 0.01$; no sigma parameters were $> 100$; and the range parameter was of a reasonable size. Models that did not converge were excluded from further consideration.

For models that passed all the sanity checks, I used the **sdmTMBextra** predict_mle_mcmc() function to generate MCMC-based randomized-quantile residuals, then examined the Q-Q plots for evidence of deviations from the reference distribution. I plotted the MCMC-based randomized-quantile residuals over space and time to visualize potential patterns of autocorrelation.

I tested for spatial patterns in residuals using a global Moran's I clustering analysis, which I applied across each year of the time series in order to evaluate the evidence for autocorrelation across the spatial domain

for that year (Moran 1950; Cacciapaglia et al. 2024). I ran Monte Carlo simulations of Moran's I with the mc.moran() function from the R package **spdep** (Bivand 2022), with the null hypothesis that the residual values were randomly distributed in space. The resulting Moran's I statistic for each year is an overall score of clustering for the spatial residuals across the spatial domain in the year in question. Positive Moran's I statistic values indicate spatial autocorrelation while negative values indicate negative spatial autocorrelation. P-values $< 0.05$ indicate significant clustering of spatial residuals.

I evaluated model predictive skill (the predictive ability of the model for new observations; Anderson *et al.* 2024) using the cross validation function sdmTMB_cv(). This function measures model predictive skill by holding out subsets of the data in turn and using each as a test set. These subsets of data are termed "folds". To compare models, I performed cross validation with 10 randomly arranged folds for each model before extracting the model's summed log-likelihood value, which represents the model's predictive density. Predictive density values closer to zero indicate better out-of-sample predictive skill. I calculated Root Mean Square Error (RMSE) and Mean Absolute Error (MAE) based on the predictive values.

## Model specification

I modeled the number of crab per $km^2$ caught in the survey with three model structures, all of which are appropriate for modeling data with many zeros and positive continuous values: Tweedie with a log link, delta-gamma with a logit link for the binomial distribution and a log link for the gamma distribution, and delta-lognormal with a logit link for the binomial distribution and a log link for the lognormal distribution. The delta-gamma and delta-lognormal families are delta-models, which are frequently used in fisheries to separately model the encounter probability and the positive catch rate in survey time series (Pennington 1983; Thorson et al. 2021). Here, the first component estimates the effects on encounter probability (binomial, zero versus non-zero number of crab per $km^2$), while the second component (gamma or lognormal distribution) estimates effects on the positive response variable (non-zero number of crab per $km^2$).

I used model diagnostics including Q-Q plots of MCMC-based randomized-quantile residuals, and predictive density, RMSE, and MAE values derived from cross-validation, to select the best model for each survey data set. All six models (Tweedie/year + survey, Tweedie/year + survey + depth, delta-gamma/year + survey, delta-gamma/year + survey + depth, delta-lognormal/year + survey, delta-lognormal/year + survey + depth) converged.

## Predictions

The stock assessment model for Norton Sound red king crab currently uses design-based estimates of abundance from the ADF&G survey and NOAA NBS survey that are calculated using a smaller spatial area (maximum 5,641 $nm^2$ or 19,348 $km^2$) than are those for the NOAA Norton Sound survey (7,600 $nm^2$ or 26,067 $km^2$), and the previous stock assessment author suggested using only survey stations that fall within the ADF&G survey sampling area for abundance estimation (Hamazaki 2024). To explore the implications of estimating abundance over different spatial scales, I generated prediction grids with the prediction area defined to include either all survey stations sampled in all three surveys (Figure 8; area = 76,487 $km^2$), or the prediction area defined to include only the survey stations sampled in the ADF&G trawl survey since 2010 (Figure 9; area = 32,413 $km^2$). Note that the area of the smaller prediction grid is still larger than the area over which the design-based estimates of abundance currently used in the stock assessment model are currently calculated, as those calculations leave out some southern and closer to shore areas of Norton Sound (Figure d1 in Hamazaki 2024). I specified the spatial resolution of the predictions as 10 $km^2$.

I used the **sdmTMB** predict() function to generate predictions about crab abundance from each model over the prediction grid. To estimate uncertainty in the spatiotemporal predictions, I used simulations from the joint precision matrix to generate 100 estimates, then calculated the coefficients of variation for each year in the time series.

### Indices of abundance

I used the **sdmTMB** get_index() function to calculate total abundance estimates and standard errors from each model, then plotted these model-based indices with the design-based indices currently used in the stock assessment model for visual comparison.

### Stock assessment model

The Norton Sound red king crab stock assessment model, which uses the Generalized size-structured Model for Assessing Crustacean Stocks (GMACS) framework, is described in detail elsewhere (Stern and Palof 2025; Hamazaki 2024). The base version of the model used in this analysis is similar to the new base model (24.0b) presented at the Crab Plan Team meeting in May 2025, with one alteration: a prior borrowed from the Bristol Bay red king crab model was used for the winter commercial fishery fully selected fishing mortality ($F$), which has the effect of avoiding the likely unrealistically large $F$ values estimated by model 24.0b. The model using this prior is termed 24.0b6, and will be presented formally at the Crab Plan Team meeting in November 2025.

The first alternative model presented here is 24.0b6a, which is model 24.0b6 with the ADF&G and NOAA NBS trawl survey design-based indices removed and replaced by a model-based index combining information from both surveys; the NOAA Norton Sound survey design-based index is retained. Catchability is fixed at 1 for the model-based index and estimated for the design-based index. The second alternative model is 24.0b6b, which is model 24.0b6a with the NOAA Norton Sound survey design-based index removed. Catchability is fixed at 1 for the model-based index. Other models not shown explored estimating catchability for the model-based index and yielded estimated catchabilities greater than 1; revisiting catchability estimation is a priority for future research.

Retrospective analyses for model estimates of mature male biomass (MMB) were performed by sequentially removing each of the most recent 9 years of data, fitting the model, and recorded estimated MMB. Comparing the estimated MMB time series as each year of data is removed permits identification of retrospective patterns, in which estimates show consistent deviations with each "peel" (removal of a year of data).

## Results

### Spatiotemporal model diagnostics

The quantile-quantile plots generated using MCMC-based randomized-quantile residuals indicate potential issues with the models using the Tweedie and delta lognormal distributions in the tails, while the residuals for the models using the delta gamma distribution appear to deviate less from linearity (Figures 10 - 15).

The spatial distributions of MCMC-based randomized-quantile for the models are plotted in Figures 16 - 21. Using visual inspection, there do not appear to be consistent spatial patterns in residuals for any of the models.

The Moran's I clustering analysis yielded evidence of spatial autocorrelation in the residuals in 1 of the 16 years in the time series for the Tweedie model with year and survey identity fixed effects; 1 year for the Tweedie model with year, survey identity, and depth fixed effects; 1 year for the delta gamma model with year and survey identity fixed effects; 2 years for the delta gamma model with year, survey identity, and depth fixed effects; 2 years for the delta lognormal model with year and survey identity fixed effects; and 4 years for the delta lognormal model with year, survey identity, and depth fixed effects (Tables 2 - 4).

The predictive density value of the model using the delta lognormal distribution with year, survey identity, and depth fixed effects is closest to zero, indicating that this model has the best out-of-sample predictive skill of the models evaluated (Table 1). The predictive density values of the models using the Tweedie distribution

are the farthest from zero compared to the models using the same fixed effects, indicating that models using the Tweedie distribution have the poorest out-of-sample predictive skill of the models compared.

Root mean square error (RMSE) values are similar for the delta gamma and delta lognormal models with the same fixed effects, but much higher for the models using the Tweedie distribution. Mean absolute error (MAE) values are lower for the delta gamma than for the delta lognormal models with the same fixed effects, while the models using the Tweedie distribution again have higher values compared to the other models (Table 1).

Model diagnostics do not clearly indicate a best model. While the models using the Tweedie distribution did not perform as well as the other models by multiple measures, the distinction between the models using the delta gamma versus delta lognormal distributions is less clear cut. I chose the model using the delta gamma distribution with year, survey identity, and depth fixed effects as the model to produce the index used in the stock assessment model. Although this model did not have the best out-of-sample predictive skill of the models evaluated, I thought the Q-Q plots indicated fewer issues with the models using the delta gamma distribution than with the models using the Tweedie and delta lognormal distributions. Of the models using the delta gamma distribution, the model that included depth as a fixed effect had better predictive skill than the model that did not include depth. Only results from the models using the delta gamma or the delta lognormal distribution are shown below.

## Spatiotemporal model predicted abundance

The spatial distribution of model-predicted crab abundance for each model is shown in Figures 22 - 29 and appears to be similar among the models. Uncertainty in the predictions is displayed in Figures 30 - 33 and appears to be lower for the models using the delta lognormal distribution than for the models using the delta gamma distribution, at least in some years.

## Model-based indices of abundance compared to design-based index of abundance

The model-based indices generated using models that do not include depth as a fixed effect generally estimate higher abundance than those including depth, and also appear to show more year-to-year variability in abundance (Figures 34 - 37). Indices calculated using abundance predicted across the smaller prediction grid generally estimated lower abundance than indices calculated across the larger prediction grid. I decided to use an index calculated using the larger prediction grid in the stock assessment model due to concern about underestimating the scale of the population, although this decision may be revisited in future. For indices generated using the larger prediction grid, model abundance estimates fall within the uncertainty interval for the design-based abundance estimates for all years for the model using the delta gamma distribution and including depth, while the models using the delta lognormal distribution, and the delta gamma distribution model that excludes depth, all produce abundance estimates outside the design-based abundance estimate uncertainty interval in at least one year.

## Stock assessment model

### Fits

Fits to catch time series are unchanged by the use of a model-based index in the stock assessment model, and fits to size composition data change only slightly (Table 5). Fits to the three time blocks of the standardized fishery CPUE index vary among the models, with the models using the model-based index showing slightly better fits for the earliest time block and worse fits for the two later time blocks (Figures 38 - 40). The fit to the NOAA Norton Sound survey design-based index is worse when the model-based index is included, and the fit to the model-based index is slightly worse when the design-based index is excluded (Figures 41 - 42).

### Retrospective patterns

Using the spatiotemporal model-based index in the stock assessment model along with the NOAA Norton Sound survey design-based index of abundance led to a less extreme retrospective pattern compared to using the three design-based survey indices (Figures 43 and 44; Mohn's $\rho$ value reduced from 0.188 to 0.153). Using only the spatiotemporal model-based index further reduced the retrospective pattern (Figure 45; Mohn's $\rho$ = 0.146).

### Reference points

Estimated mature male biomass is lower for the models using the spatiotemporal model-based index than the model using only design-based indices across the time series (Figure 46). While estimated stock status is similar or higher for the models using the model-based index compared to the model using only design-based indices, the overall reduced scale of the population leads to lower recommended harvest (Table 6).

## Conclusions

Developing a model-based index using data from more than one survey has been a long-standing goal for the Norton Sound red king crab stock and is accomplished here. The NOAA Norton Sound trawl survey data, collected in 1976-1991, could not be included in the spatiotemporal models due to lack of temporal overlap with the other survey time series, and feedback is requested on whether to drop this time series from the stock assessment model, continue using the design-based index, or use the previously-developed model-based index for this survey (Stern 2025). Given that the NOAA NBS and ADF&G trawl surveys are the surveys expected to continue in future, the development of a model-based index incorporating both survey time series is a useful step for the Norton Sound red king crab stock assessment. New data from the 2025 NOAA NBS survey will be included in the model-based index when they are available. The ADF&G survey did not occur in 2025 but is expected to occur in 2026.

The model-based index selected to be used in the stock assessment model, derived from a spatiotemporal model using the delta gamma distribution with year, survey identity, and depth as fixed effects, shows a reasonable fit to the design-based survey indices. The addition of more years in which both surveys occurred, beyond the four currently available, would likely improve the accuracy of model estimates, and should be prioritized once the timing of the next NOAA NBS survey is known.

It is unclear whether using the spatiotemporal model-based index improves the performance of the stock assessment model. The model-based approach provides the ability to account for spatial variation and potential covariates such as depth in the index standardization process, which may reduce index variability. Using the model-based index in the stock assessment led to a less extreme retrospective pattern in mature male biomass, indicating an improved ability of the model to predict biomass for the terminal year. However, fits for the models using the model-based index did not seem to outperform the fit for the model using design-based indices. Future work will include additional comparisons of stock assessment model performance.

## Acknowledgements

I thank the members of the North Pacific Fishery Management Council Crab Plan Team, as well as Chris Siddon and Alex Reich of ADF&G, for their helpful feedback on this work. I thank Lewis Barnett of NOAA for providing invaluable advice on the development of the spatiotemporal models.

# References


Anderson SC (2025) sdmTMBextra: Extra Functions for Working with 'sdmTMB' Models. R package version 0.0.4, commit 63f236912e12ce78b5a0529eedf1e11cb93d0a10, https://github.com/pbs-assess/sdmTMBextra.

Anderson SC, Ward EJ, English PA, Barnett LAK (2022) sdmTMB: An R package for fast, flexible, and user-friendly generalized linear mixed effects models with spatial and spatiotemporal random fields. bioRxiv, *2022.03.24.485545*. doi:10.1101/2022.03.24.485545.

Anderson SC, Ward EJ, English PA, Barnett LAK, Thorson JT (2024) Cross-validation for model evaluation and comparison. Retrieved from https://pbs-assess.github.io/sdmTMB/articles/cross-validation.html.

Barbeaux SJ, Barnett L, Hulson P, Nielsen J, Shotwell SK, Siddon E, Spies I (2024) Assessment of the Pacific cod stock in the Eastern Bering Sea. In: Stock Assessment and Fishery Evaluation report for the Groundfish Resources of the Bering Sea/Aleutian Islands regions. North Pacific Fishery Management Council, Anchorage, AK. PDF.

Bivand RS. 2022. spdep: Spatial Dependence: Weighting Schemes, Statistics. R Package Version 1.2-1, https://CRAN.R-project.org/package=spdep.

Cacciapaglia C, Brooks EN, Adams CF, Legault CM, Perretti CT, Hart D (2024) Developing workflow and diagnostics for model selection of a vector autoregressive spatiotemporal (VAST) model in comparison to design-based indices. Fisheries Research 275:107009.

Chen J, Gao J, Zhang F (2024) Spatiotemporal model improves survey indices for witch flounder stock assessment in the Grand Banks. Canadian Journal of Fisheries and Aquatic Sciences 81:459–487 doi:10.1139/cjfas-2023-0101.

Commander CJC, Barnett LAK, Ward EJ, Anderson SC, Essington TE (2022) The shadow model: how and why small choices in spatially explicit species distribution models affect predictions. PeerJ 10:e12783. doi:10.7717/peerj.12783.

CPT (2021) Crab Plan Team report, January 2021. North Pacific Fishery Management Council, Anchorage, AK. PDF.

DeFilippo L, Kotwicki S, Barnett L, Richar J, Litzow MA, Stockhausen WT, Palof K (2023) Evaluating the impacts of reduced sampling density in a systematic fisheries-independent survey design. Frontiers in Marine Science 10:1219283. doi:10.3389/fmars.2023.1219283.

Hamazaki T (2024) Norton Sound red king crab stock assessment for the fishing year 2024. In: Stock Assessment and Fishery Evaluation Report for the King and Tanner Crab Fisheries of the Bering Sea and Aleutian Islands: 2024 Final Crab SAFE. North Pacific Fishery Management Council, Anchorage AK. PDF.

Hamazaki T, Zheng J (2021) Norton Sound Red King Crab Stock Assessment for the fishing year 2021. In: Stock Assessment and Fishery Evaluation Report for the King and Tanner Crab Fisheries of the Bering Sea and Aleutian Islands: 2021 Final Crab SAFE. North Pacific Fishery Management Council, Anchorage AK. PDF.

Hartig F (2022) DHARMa: Residual Diagnostics for Hierarchical (Multi-Level/Mixed) Regression Models. R package version 0.4.6, https://CRAN.R-project.org/package=DHARMa.

Ianelli J, Webber D, Zheng J, Letaw A (2017) Saint Matthew Island blue king crab stock assessment 2017. In: Stock Assessment and Fishery Evaluation Report for the King and Tanner Crab Fisheries of the Bering Sea and Aleutian Islands: 2017 Final Crab SAFE. North Pacific Fishery Management Council, Anchorage AK.

Ianelli J, Honkalehto T, Wassermann S, McCarthy A, Steinessen S, McGilliard C, Siddon E. (2024) Assessment of walleye pollock in the eastern Bering Sea. In: Stock Assessment and Fishery Evaluation report for the Groundfish Resources of the Bering Sea/Aleutian Islands regions. North Pacific Fishery Management Council, Anchorage, AK. PDF.

Lindgren F (2023) fmesher: Triangle Meshes and Related Geometry Tools. R package version 0.1.2, https://CRAN.R-project.org/package=fmesher.

Lindgren F, Rue H, Lindström J (2011). An explicit link between Gaussian fields and Gaussian Markov random fields: the stochastic partial differential equation approach. Journal of the Royal Statistical Society B 73:423–498. doi:10.1111/j.1467-9868.2011.00777.x.

Maunder MN, Punt AE (2004) Standardizing catch and effort data: a review of recent approaches. Fisheries Research 70:141–159. doi:10.1016/j.fishres.2004.08.002.

Menard J, Leon JM, Bell J, Neff L, Clark K (2022) 2021 annual management report: Norton Sound-Port Clarence area and Arctic-Kotzebue management areas. Alaska Department of Fish and Game, Division of Commercial Fisheries, Fishery Management Report No. 22-27. PDF.

Moran PA (1950) Notes on continuous stochastic phenomena. Biometrika 37:17–23. doi:10.1093/biomet/37.1-2.17.

Patterson K, Cook R, Darby C, Gavaris S, Kell L, Lewy P, Mesnil B, Punt A, Restrepo V, Skagen DW, Stefansoon G (2001) Estimating uncertainty in fish stock assessment and forecasting. Fish and Fisheries 2:125-157. doi:10.1046/j.1467-2960.2001.00042.x.

Pennington M (1983) Efficient estimators of abundance, for fish and plankton surveys. Biometrics 39:281-286. doi:10.2307/2530830.

R Core Team (2024) R: A Language and Environment for Statistical Computing. R Foundation for Statistical Computing, Vienna, Austria. https://www.R-project.org/.

Shelton AO, Thorson JT, Ward EJ, Feist BE (2014) Spatial semiparametric models improve estimates of species abundance and distribution. Canadian Journal of Fisheries and Aquatic Sciences 71:1655–1666 doi:10.1139/cjfas-2013-0508.

SSC (2017) Scientific and Statistical Committee report to the North Pacific Fishery Management Council, October 2nd-4th, 2017. North Pacific Fishery Management Council, Anchorage, AK. PDF.

SSC (2020) Scientific and Statistical Committee final report to the North Pacific Fishery Management Council, September 28th-October 2nd, 2020. North Pacific Fishery Management Council, Anchorage, AK. PDF

SSC (2021) Scientific and Statistical Committee report to the North Pacific Fishery Management Council, February 1st-5th, 2021. North Pacific Fishery Management Council, Anchorage, AK. PDF.

Stern (2025) Spatiotemporal model-based survey indices of abundance for Norton Sound red king crab. North Pacific Fishery Management Council, Anchorage AK. PDF.

Stern and Palof (2025) Proposed models for the 2025 Norton Sound red king crab stock assessment. North Pacific Fishery Management Council, Anchorage AK. PDF.

Stockhausen WT (2024) 2024 stock assessment and fishery evaluation report for the Tanner crab fisheries of the Bering Sea and Aleutians Islands regions. In: Stock Assessment and Fishery Evaluation Report for the King and Tanner Crab Fisheries of the Bering Sea and Aleutian Islands: 2024 Final Crab SAFE. North Pacific Fishery Management Council, Anchorage AK. PDF.

Thorson JT (2019) Guidance for decisions using the vector autoregressive spatio-temporal (VAST) package in stock, ecosystem, habitat, and climate assessments. Fisheries Research 210:143-161. doi:10.1016/j.fishres.2018.10.013.

Thorson JT, Barnett LAK (2017) Comparing estimates of abundance trends and distribution shifts using single- and multispecies models of fishes and biogenic habitat. ICES Journal of Marine Science 74:1311–1321. doi:10.1093/icesjms/fsw193.

Thorson JT, Cunningham CJ, Jorgensen E, Havron A, Hulson P-JF, Monnahan CC, von Szalay P (2021) The surprising sensitivity of index scale to delta-model assumptions: recommendations for model-based index standardization. Fisheries Research 233:105745. doi:10.1016/j.fishres.2020.105745.

Thorson JT, Maunder MN, Punt AE (2020) The development of spatio-temporal models of fishery catch-per-unit effort data to derive indices of relative abundance. Fisheries Research 230:105611. doi:10.1016/j.fishres.2020.105611.

Thorson JT, Shelton AO, Ward EJ, Skaug HJ (2015) Geostatistical delta-generalized linear mixed models improve precision for estimated abundance indices for West Coast groundfishes. ICES Journal of Marine Science 72:1297-1310. doi:10.1093/icesjms/fsu243.

Yalcin S, Anderson SC, Regular PM, English PA (2023) Exploring the limits of spatiotemporal and design-based index standardization under reduced survey coverage. ICES Journal of Marine Sciences 80:2368-2379. doi:10.1093/icesjms/fsad155.

# Tables

Table 1: Norton Sound red king crab trawl survey fitted model predictive density (log-likelihood) values, estimated using sdmTMB cross-validation with 10 folds, for models fitted with spatial random fields estimated as independent and identically distributed (IID). Predictive density values closer to zero represent better out-of-sample predictive skill. Root mean square error (RMSE) and mean absolute error (MAE) calculated across the entire dataset (rather than by fold) are also shown. Models were fitted to the combined time series of the Alaska Department of Fish and Game (ADF&G) and National Atmospheric and Oceanic Administration (NOAA) Northern Bering Sea (NBS) trawl surveys.

| Distribution | Fixed effects | Log-likelihood | RMSE | MAE |
|---|---|---|---|---|
| Tweedie | year, survey | -3788.48 | 622.14 | 142.21 |
| Tweedie | year, survey, depth | -3744.84 | 856.23 | 153.71 |
| delta lognormal | year, survey | -3535.75 | 438.52 | 126.19 |
| delta lognormal | year, survey, depth | -3504.84 | 444.73 | 129.31 |
| delta gamma | year, survey | -3752.47 | 439.43 | 123.39 |
| delta gamma | year, survey, depth | -3702.16 | 445.23 | 126.48 |

Table 2: Clustering analyses for spatiotemporal models using the Tweedie distribution fitted to the Alaska Department of Fish and Game (ADF&G) and NOAA Northern Bering Sea trawl survey time series for Norton Sound red king crab. The Moran's I statistic for each year is an overall score of clustering for the spatial residuals across the spatial domain in that year. Positive Moran's I statistic values indicate spatial autocorrelation while negative values indicate negative spatial autocorrelation. P-values $< 0.05$ indicate significant clustering of spatial residuals.

| Distribution | Fixed effects | Year | Moran's I statistic | p-value |
|---|---|---|---|---|
| Tweedie | year, survey | 1996 | 0.016 | 0.224 |
| Tweedie | year, survey | 1999 | 0.003 | 0.315 |
| Tweedie | year, survey | 2002 | -0.116 | 0.993 |
| Tweedie | year, survey | 2006 | 0.135 | 0.003 |
| Tweedie | year, survey | 2008 | 0.018 | 0.223 |
| Tweedie | year, survey | 2010 | -0.079 | 0.793 |
| Tweedie | year, survey | 2011 | -0.045 | 0.725 |
| Tweedie | year, survey | 2014 | 0.027 | 0.185 |
| Tweedie | year, survey | 2017 | -0.018 | 0.562 |
| Tweedie | year, survey | 2018 | 0.002 | 0.297 |
| Tweedie | year, survey | 2019 | -0.059 | 0.858 |
| Tweedie | year, survey | 2020 | -0.077 | 0.889 |
| Tweedie | year, survey | 2021 | -0.074 | 0.934 |
| Tweedie | year, survey | 2022 | 0.000 | 0.274 |
| Tweedie | year, survey | 2023 | 0.019 | 0.200 |
| Tweedie | year, survey | 2024 | -0.001 | 0.257 |
| Tweedie | year, survey, depth | 1996 | 0.053 | 0.087 |
| Tweedie | year, survey, depth | 1999 | 0.173 | 0.005 |
| Tweedie | year, survey, depth | 2002 | -0.022 | 0.465 |
| Tweedie | year, survey, depth | 2006 | 0.040 | 0.120 |
| Tweedie | year, survey, depth | 2008 | -0.010 | 0.430 |
| Tweedie | year, survey, depth | 2010 | 0.082 | 0.056 |
| Tweedie | year, survey, depth | 2011 | 0.037 | 0.142 |
| Tweedie | year, survey, depth | 2014 | -0.056 | 0.709 |
| Tweedie | year, survey, depth | 2017 | 0.062 | 0.065 |
| Tweedie | year, survey, depth | 2018 | -0.002 | 0.370 |
| Tweedie | year, survey, depth | 2019 | 0.011 | 0.270 |
| Tweedie | year, survey, depth | 2020 | -0.079 | 0.917 |
| Tweedie | year, survey, depth | 2021 | -0.026 | 0.605 |
| Tweedie | year, survey, depth | 2022 | 0.014 | 0.211 |
| Tweedie | year, survey, depth | 2023 | 0.037 | 0.109 |
| Tweedie | year, survey, depth | 2024 | 0.021 | 0.196 |

Table 3: Clustering analyses for spatiotemporal models using the delta gamma distribution fitted to the Alaska Department of Fish and Game (ADF&G) and NOAA Northern Bering Sea trawl survey time series for Norton Sound red king crab. The Moran's I statistic for each year is an overall score of clustering for the spatial residuals across the spatial domain in that year. Positive Moran's I statistic values indicate spatial autocorrelation while negative values indicate negative spatial autocorrelation. P-values $< 0.05$ indicate significant clustering of spatial residuals.

| Distribution | Fixed effects | Year | Moran's I statistic | p-value |
|---|---|---|---|---|
| delta gamma | year, survey | 1996 | -0.049 | 0.693 |
| delta gamma | year, survey | 1999 | -0.019 | 0.452 |
| delta gamma | year, survey | 2002 | -0.000 | 0.336 |
| delta gamma | year, survey | 2006 | 0.048 | 0.090 |
| delta gamma | year, survey | 2008 | 0.005 | 0.313 |
| delta gamma | year, survey | 2010 | 0.113 | 0.015 |
| delta gamma | year, survey | 2011 | 0.028 | 0.195 |
| delta gamma | year, survey | 2014 | 0.021 | 0.182 |
| delta gamma | year, survey | 2017 | -0.060 | 0.886 |
| delta gamma | year, survey | 2018 | -0.039 | 0.646 |
| delta gamma | year, survey | 2019 | -0.010 | 0.445 |
| delta gamma | year, survey | 2020 | -0.043 | 0.682 |
| delta gamma | year, survey | 2021 | -0.077 | 0.945 |
| delta gamma | year, survey | 2022 | -0.061 | 0.651 |
| delta gamma | year, survey | 2023 | -0.034 | 0.692 |
| delta gamma | year, survey | 2024 | -0.036 | 0.508 |
| delta gamma | year, survey, depth | 1996 | 0.065 | 0.076 |
| delta gamma | year, survey, depth | 1999 | 0.040 | 0.130 |
| delta gamma | year, survey, depth | 2002 | 0.127 | 0.006 |
| delta gamma | year, survey, depth | 2006 | -0.049 | 0.768 |
| delta gamma | year, survey, depth | 2008 | 0.013 | 0.264 |
| delta gamma | year, survey, depth | 2010 | 0.058 | 0.090 |
| delta gamma | year, survey, depth | 2011 | -0.047 | 0.741 |
| delta gamma | year, survey, depth | 2014 | 0.140 | 0.016 |
| delta gamma | year, survey, depth | 2017 | 0.016 | 0.224 |
| delta gamma | year, survey, depth | 2018 | -0.050 | 0.709 |
| delta gamma | year, survey, depth | 2019 | -0.076 | 0.955 |
| delta gamma | year, survey, depth | 2020 | -0.097 | 0.977 |
| delta gamma | year, survey, depth | 2021 | -0.111 | 0.995 |
| delta gamma | year, survey, depth | 2022 | -0.063 | 0.674 |
| delta gamma | year, survey, depth | 2023 | -0.069 | 0.925 |
| delta gamma | year, survey, depth | 2024 | 0.009 | 0.208 |

Table 4: Clustering analyses for spatiotemporal models using the delta lognormal distribution fitted to the Alaska Department of Fish and Game (ADF&G) and NOAA Northern Bering Sea trawl survey time series for Norton Sound red king crab. The Moran's I statistic for each year is an overall score of clustering for the spatial residuals across the spatial domain in that year. Positive Moran's I statistic values indicate spatial autocorrelation while negative values indicate negative spatial autocorrelation. P-values $< 0.05$ indicate significant clustering of spatial residuals.

| Distribution | Fixed effects | Year | Moran's I statistic | p-value |
|---|---|---|---|---|
| delta lognormal | year, survey | 1996 | -0.064 | 0.791 |
| delta lognormal | year, survey | 1999 | 0.007 | 0.272 |
| delta lognormal | year, survey | 2002 | 0.001 | 0.304 |
| delta lognormal | year, survey | 2006 | 0.021 | 0.222 |
| delta lognormal | year, survey | 2008 | 0.079 | 0.042 |
| delta lognormal | year, survey | 2010 | 0.017 | 0.194 |
| delta lognormal | year, survey | 2011 | -0.088 | 0.946 |
| delta lognormal | year, survey | 2014 | 0.017 | 0.218 |
| delta lognormal | year, survey | 2017 | -0.005 | 0.423 |
| delta lognormal | year, survey | 2018 | 0.056 | 0.084 |
| delta lognormal | year, survey | 2019 | 0.105 | 0.007 |
| delta lognormal | year, survey | 2020 | -0.061 | 0.820 |
| delta lognormal | year, survey | 2021 | -0.087 | 0.962 |
| delta lognormal | year, survey | 2022 | -0.015 | 0.328 |
| delta lognormal | year, survey | 2023 | 0.044 | 0.078 |
| delta lognormal | year, survey | 2024 | -0.028 | 0.452 |
| delta lognormal | year, survey, depth | 1996 | -0.043 | 0.624 |
| delta lognormal | year, survey, depth | 1999 | 0.073 | 0.067 |
| delta lognormal | year, survey, depth | 2002 | 0.037 | 0.131 |
| delta lognormal | year, survey, depth | 2006 | -0.000 | 0.323 |
| delta lognormal | year, survey, depth | 2008 | 0.096 | 0.017 |
| delta lognormal | year, survey, depth | 2010 | 0.129 | 0.018 |
| delta lognormal | year, survey, depth | 2011 | 0.013 | 0.264 |
| delta lognormal | year, survey, depth | 2014 | 0.106 | 0.033 |
| delta lognormal | year, survey, depth | 2017 | 0.017 | 0.193 |
| delta lognormal | year, survey, depth | 2018 | -0.004 | 0.363 |
| delta lognormal | year, survey, depth | 2019 | 0.090 | 0.017 |
| delta lognormal | year, survey, depth | 2020 | -0.014 | 0.451 |
| delta lognormal | year, survey, depth | 2021 | -0.072 | 0.927 |
| delta lognormal | year, survey, depth | 2022 | -0.005 | 0.274 |
| delta lognormal | year, survey, depth | 2023 | 0.012 | 0.282 |
| delta lognormal | year, survey, depth | 2024 | -0.093 | 0.913 |

Table 5: Comparisons of negative log-likelihood values for the stock assessment models. Model 24.0b6 uses design-based indices for each of the three trawl surveys, model 24.0b6a uses a design-based index for the NOAA Norton Sound trawl survey and a spatiotemporal model-based index combining data from the NOAA NBS and ADF&G trawl surveys, and model 24.0b6b uses a spatiotemporal model-based index combining data from the NOAA NBS and ADF&G trawl surveys (no design-based survey indices).

| Component | 24.0b6 | 24.0b6a | 24.0b6b |
|---|---|---|---|
| Winter comm. retained catch | -119.04 | -119.04 | -119.04 |
| Subsistence retained catch | -121.63 | -121.63 | -121.63 |
| Subsistence total catch | 0.00 | 0.00 | 0.00 |
| Summer comm. retained catch | -116.44 | -116.44 | -116.44 |
| Model-based index | | -3.88 | -3.36 |
| NMFS trawl survey 1976-1991 | -3.31 | -2.60 | |
| ADF&G trawl survey | -4.04 | | |
| NOAA NBS survey | -5.41 | | |
| Pot CPUE 1977-1992 | -2.98 | -3.13 | -3.01 |
| Pot CPUE 1993-2006 | -5.06 | -0.48 | -0.46 |
| Pot CPUE 2007-2024 | -11.33 | -1.93 | -1.91 |
| Winter com. retained size comp. | 50.97 | 50.81 | 50.72 |
| Summer com. retained size comp. | 703.56 | 703.41 | 702.71 |
| Summer com. discard size comp. | 279.74 | 279.79 | 279.81 |
| Summer com. total size comp | 216.62 | 216.75 | 216.77 |
| NMFS trawl survey size comp. | 317.70 | 316.94 | 316.53 |
| ADF&G trawl survey size comp. | 282.76 | 282.25 | 281.74 |
| NBS trawl survey size comp. | 157.33 | 157.08 | 156.99 |
| Winter pot survey size comp. | 613.77 | 611.96 | 612.64 |
| Recruitment deviations | 51.15 | 51.02 | 50.61 |
| Tagging | 1724.67 | 1724.71 | 1724.77 |
| Growth | 1724.67 | 1724.71 | 1724.77 |
| F penalty | 14.21 | 14.21 | 14.21 |
| Prior | 95.49 | 94.38 | 93.67 |
| Total | 4182.64 | 4198.18 | 4199.09 |
| Total estimated parameters | 226.00 | 225.00 | 224.00 |

Table 6: Comparisons of management measures for models 24.0b6, 24.0b6a, and 24.0b6b. Model 24.0b6 uses design-based indices for each of the three trawl surveys, model 24.0b6a uses a design-based index for the NOAA Norton Sound trawl survey and a spatiotemporal model-based index combining data from the NOAA NBS and ADF&G trawl surveys, and model 24.0b6b uses a spatiotemporal model-based index combining data from the NOAA NBS and ADF&G trawl surveys (no design-based survey indices). Biomass, OFL, and ABC are in tons.

| Component | 24.0b6 | 24.0b6a | 24.0b6b |
|---|---|---|---|
| $\text{MMB}_{2024}$ | 4642.00 | 3630.00 | 3620.00 |
| $B_{\text{MSY}}$ | 1947.00 | 1516.00 | 1414.00 |
| $MMB/B_{\text{MSY}}$ | 1.08 | 1.09 | 1.16 |
| $F_{\text{OFL}}$ | 0.18 | 0.18 | 0.18 |
| $\text{OFL}_{2024}$ | 577.00 | 456.00 | 457.00 |
| $\text{ABC}_{2024}$ | 404.00 | 319.00 | 320.00 |

## Figures

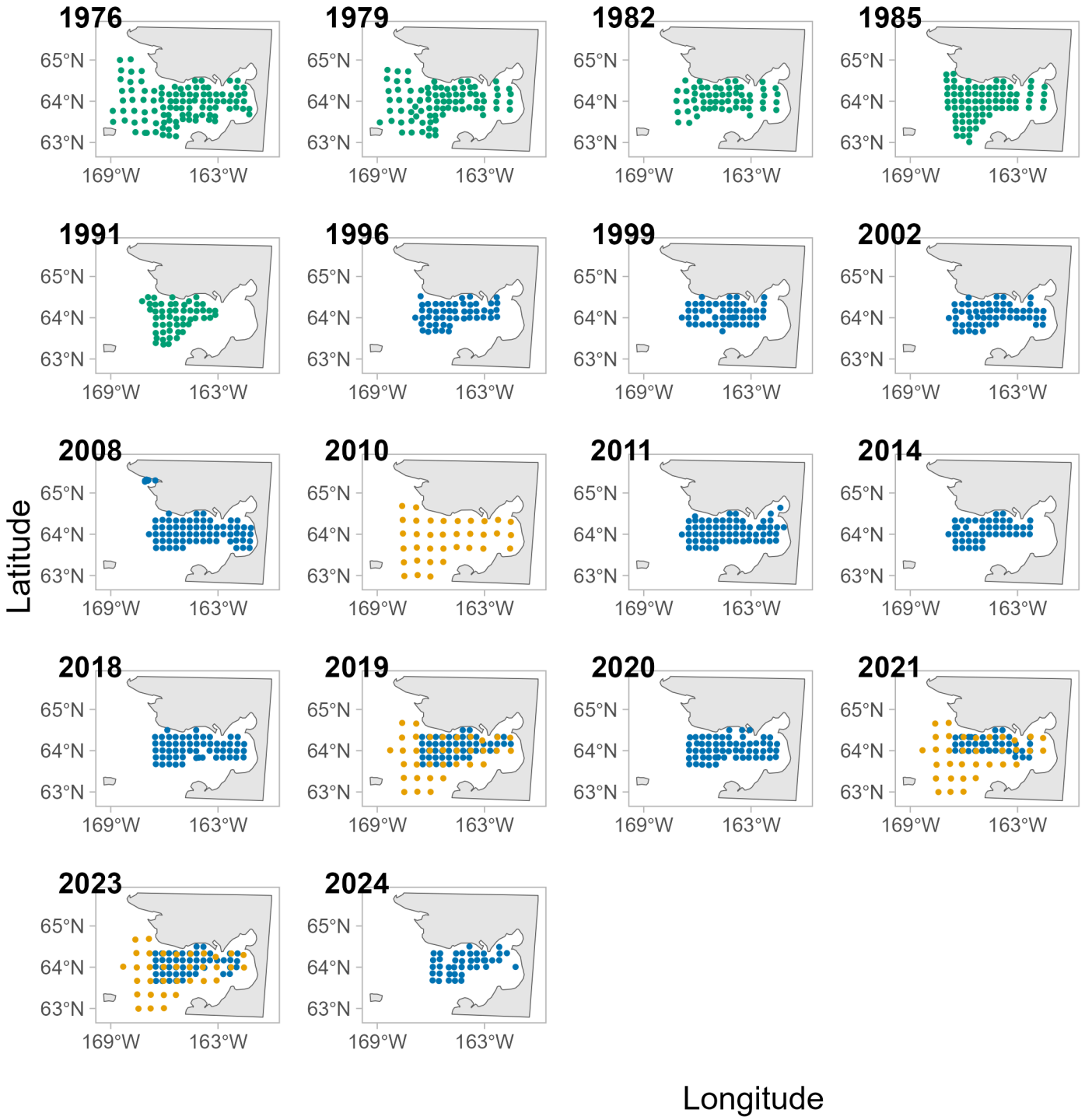


Figure 1: Survey sampling by year for the Norton Sound red king crab stock from the NOAA Norton Sound trawl survey (green), ADF&G trawl survey (blue), and NOAA Northern Bering Sea survey (gold).

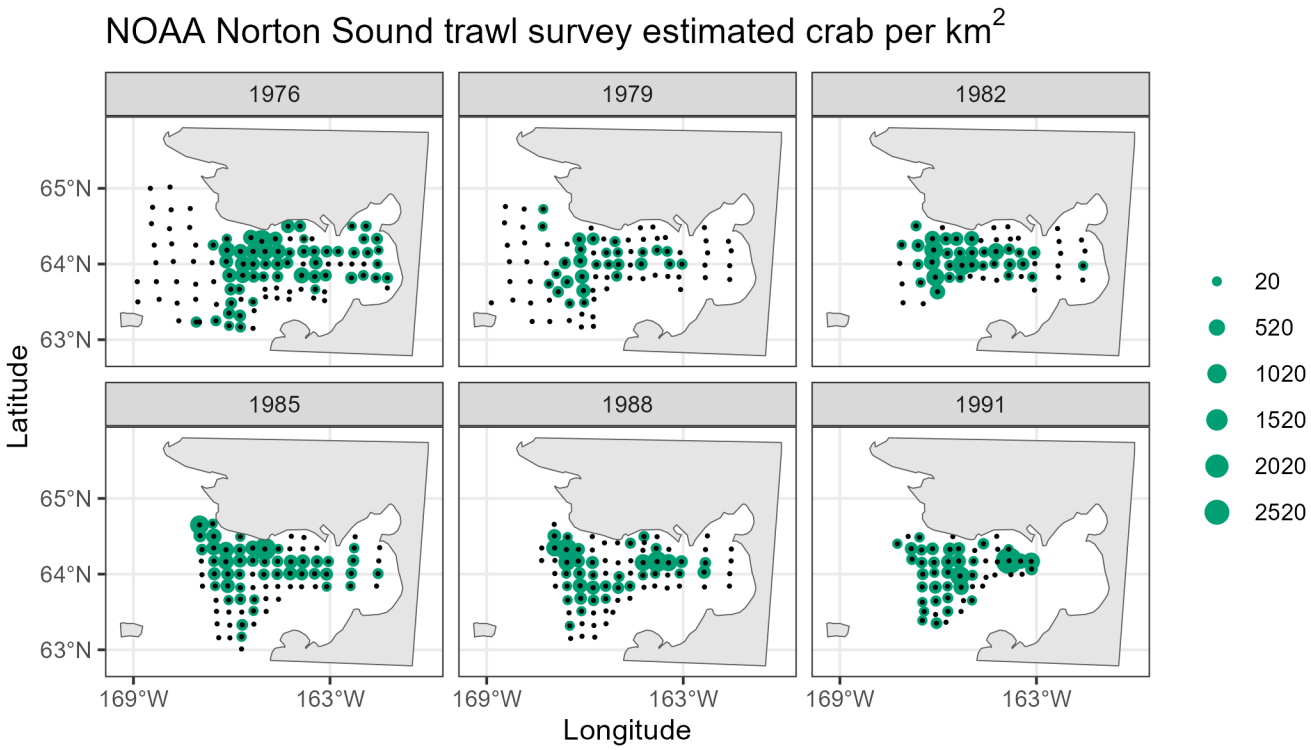


Figure 2: Estimated density in crab/km$^2$ for males $\geq$ 64 mm in carapace length by survey station in the NOAA Norton Sound trawl survey. Black points represent sampled survey stations while green points indicate estimated density.

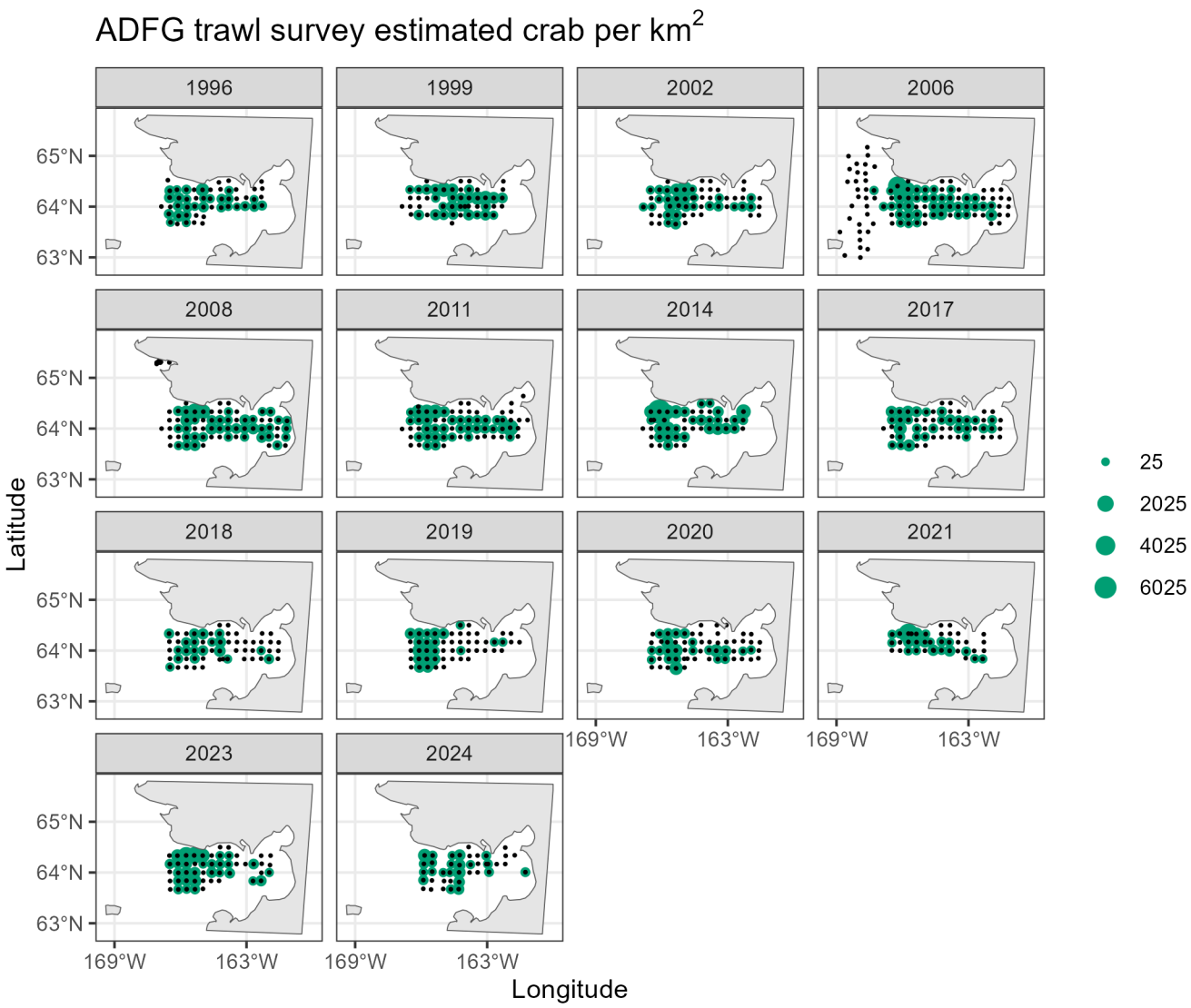


Figure 3: Estimated density in crab/km$^2$ for males $\geq$ 64 mm in carapace length by survey station in the ADF&G trawl survey. Black points represent sampled survey stations while green points indicate estimated density.

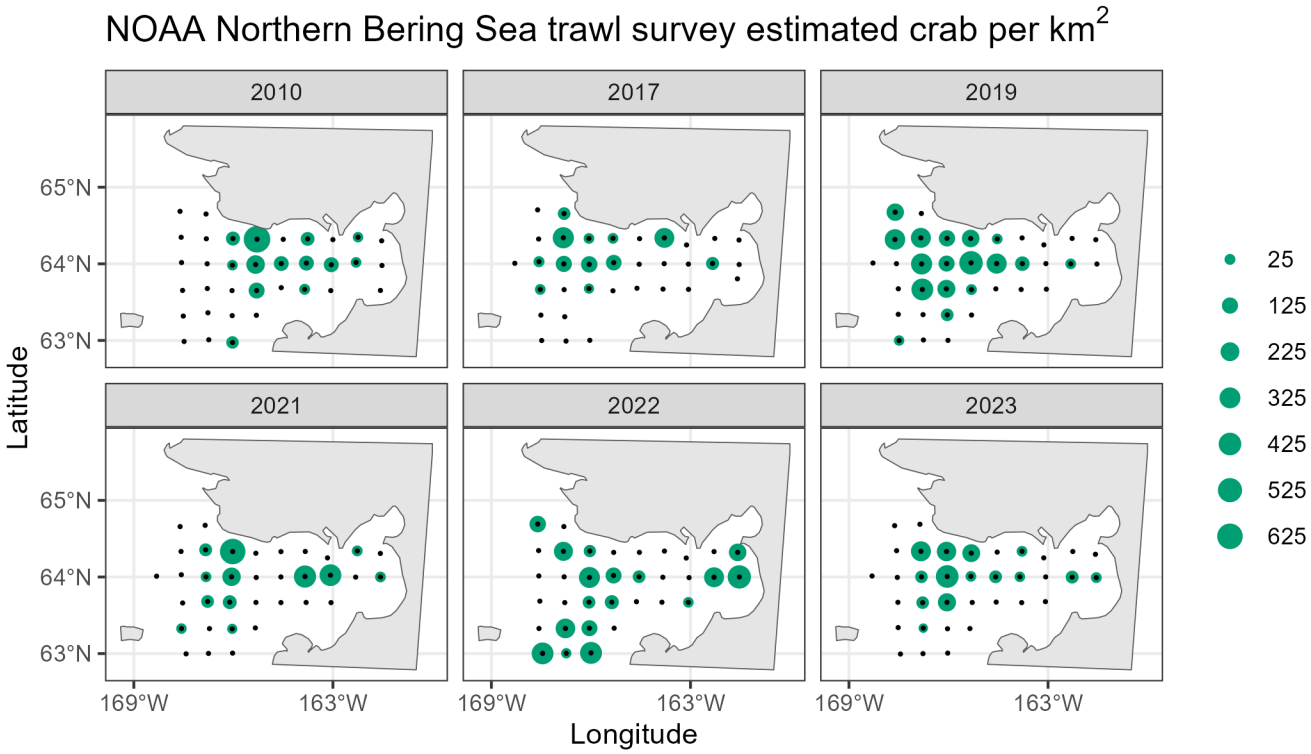


Figure 4: Estimated density in crab/km$^2$ for males $\geq$ 64 mm in carapace length by survey station in the NOAA Northern Bering Sea trawl survey. Black points represent sampled survey stations while green points indicate estimated density.

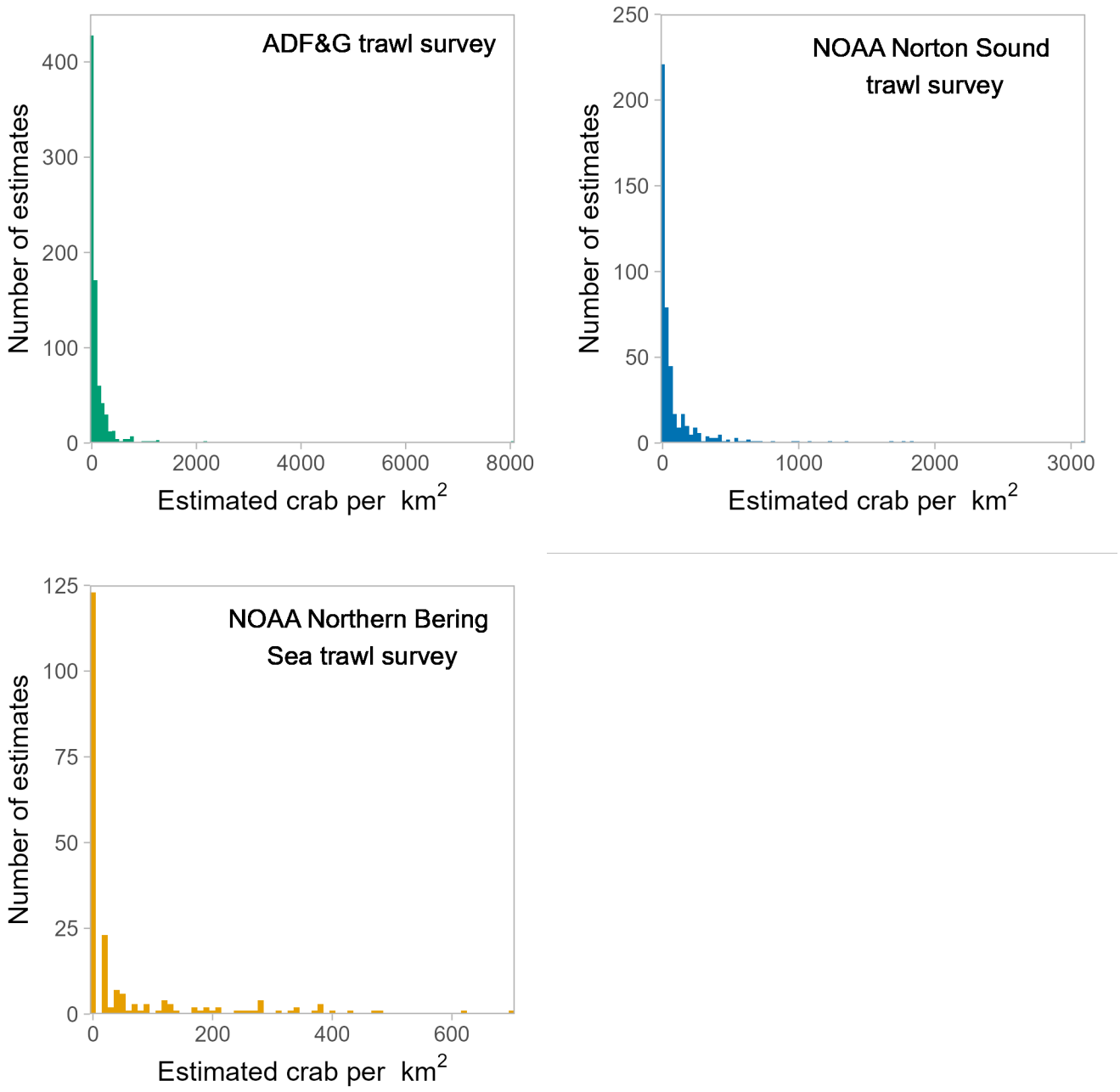


Figure 5: Distribution of density estimates (in crab/km$^2$) for males $\geq$ 64 mm in carapace length in each trawl survey time series.

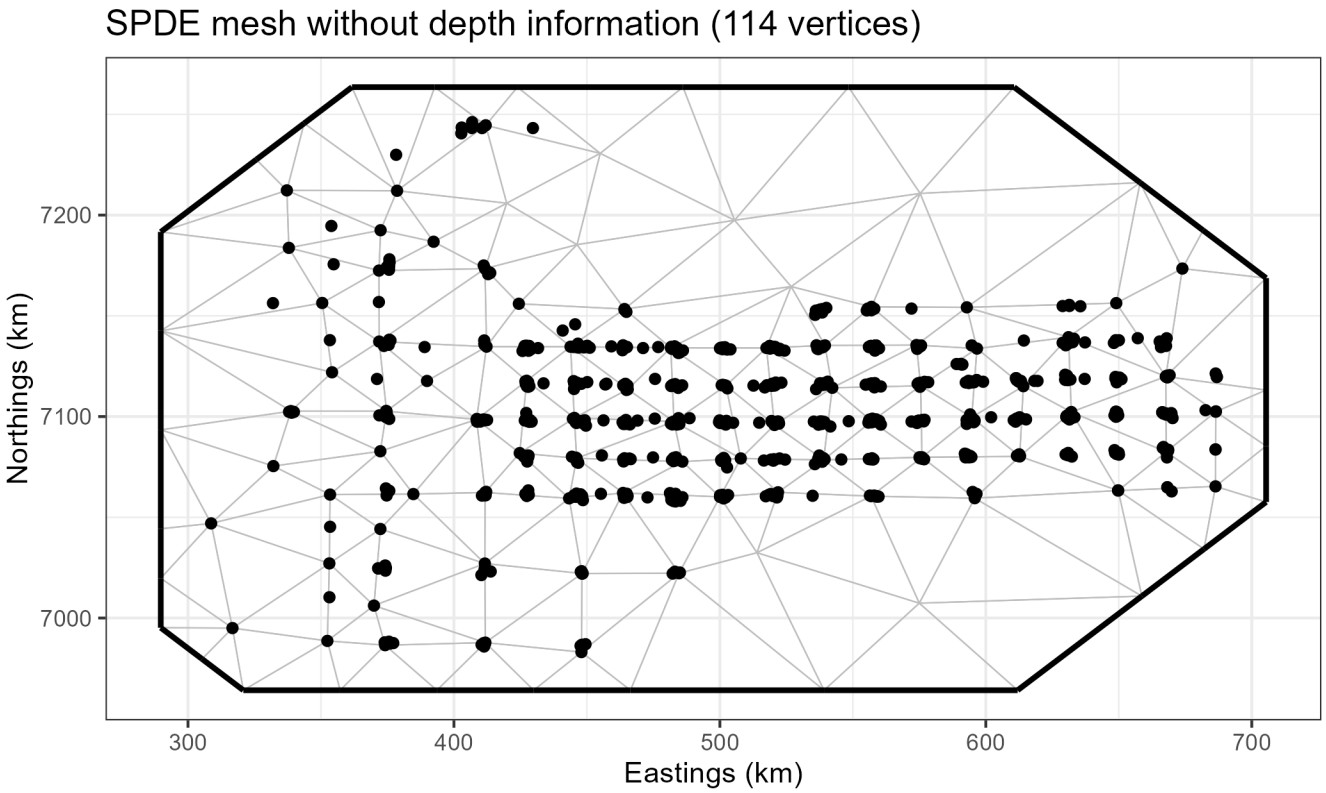


Figure 6: Spatial mesh used for fitting Norton Sound red king crab spatial models without depth included to ADF&G and NOAA NBS trawl survey data. The mesh incorporates correlation barriers based on the Norton Sound coastline. Points represent survey observations.

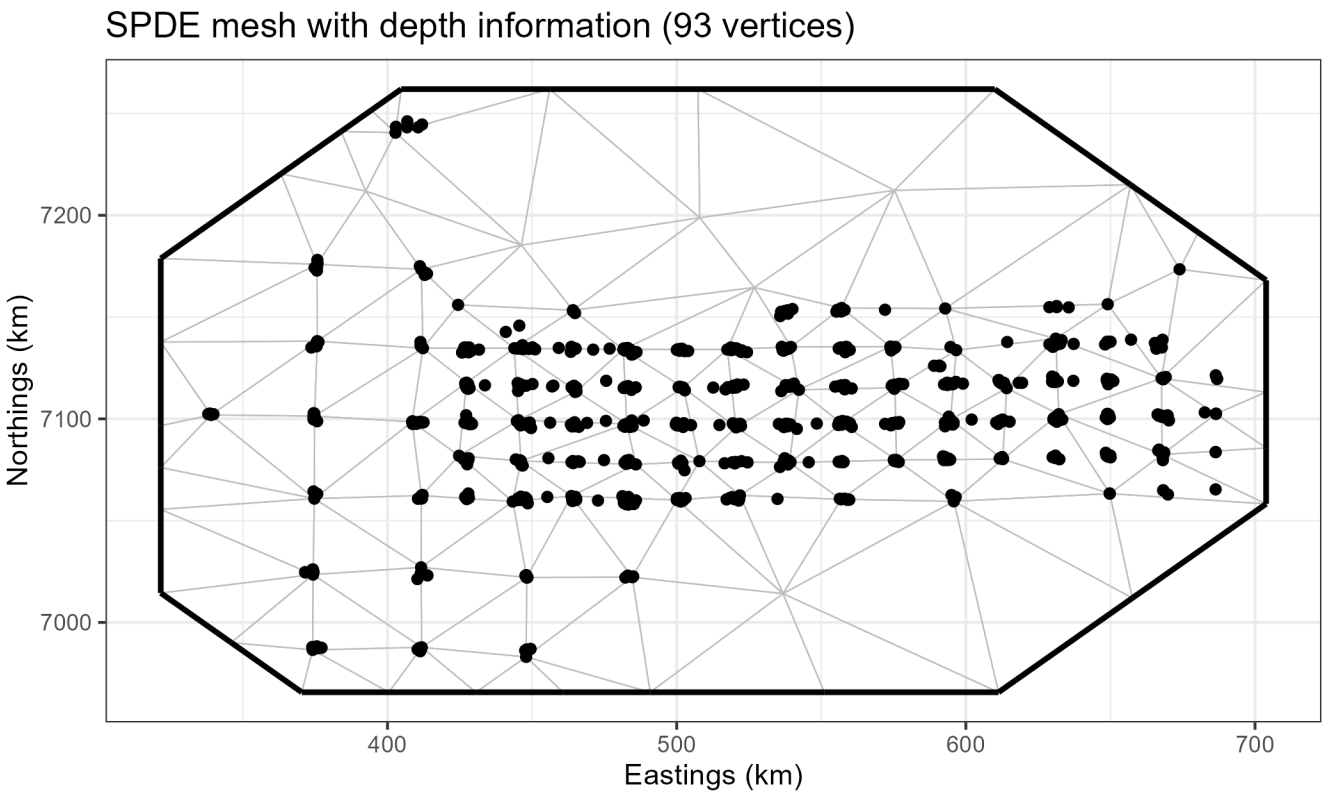


Figure 7: Spatial mesh used for fitting Norton Sound red king crab spatial models with depth included as a fixed effect to ADF&G and NOAA NBS trawl survey data. The mesh incorporates correlation barriers based on the Norton Sound coastline. Points represent survey observations with depth information available.

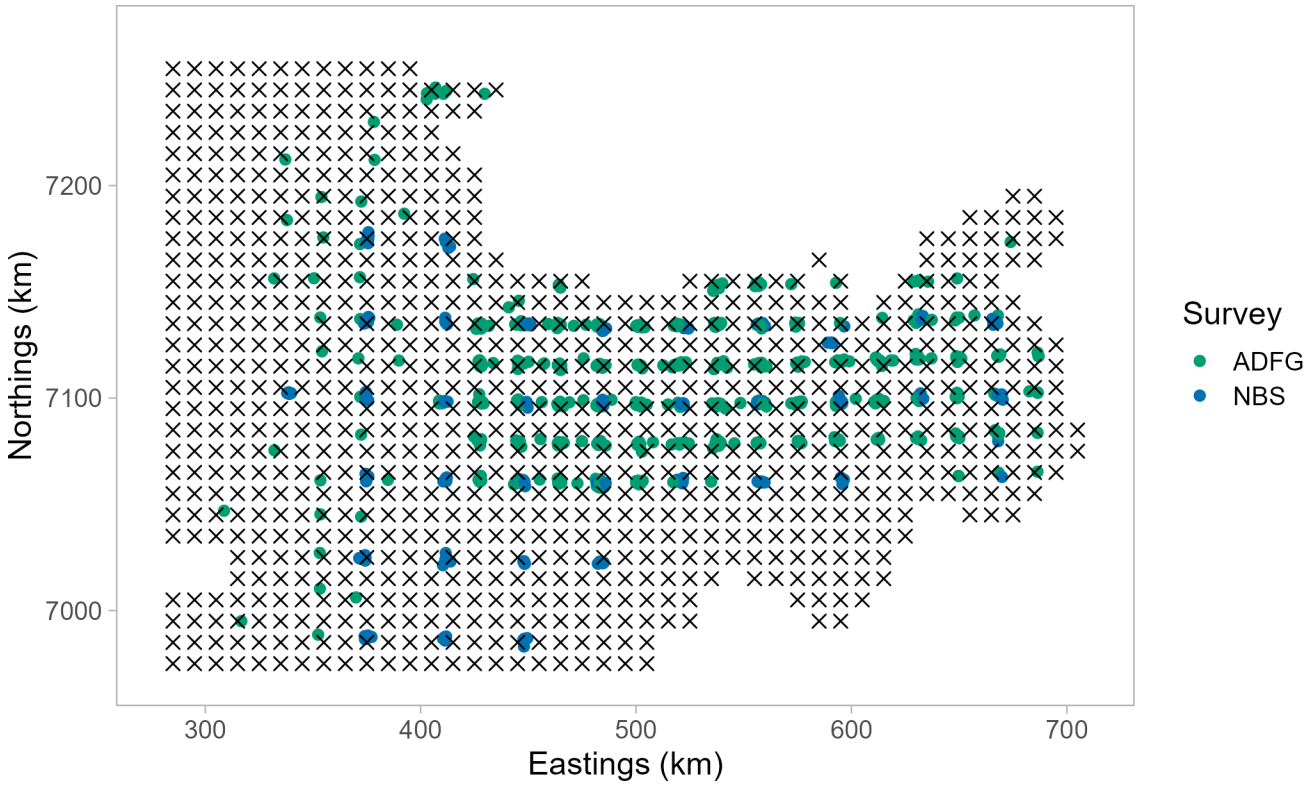


Figure 8: Larger Norton Sound prediction grid used for red king crab spatial abundance predictions. Prediction grid spatial resolution is 10 $km^2$ and the grid does not include land. Survey data from all years of the ADF&G and NOAA NBS trawl surveys are shown for comparison.

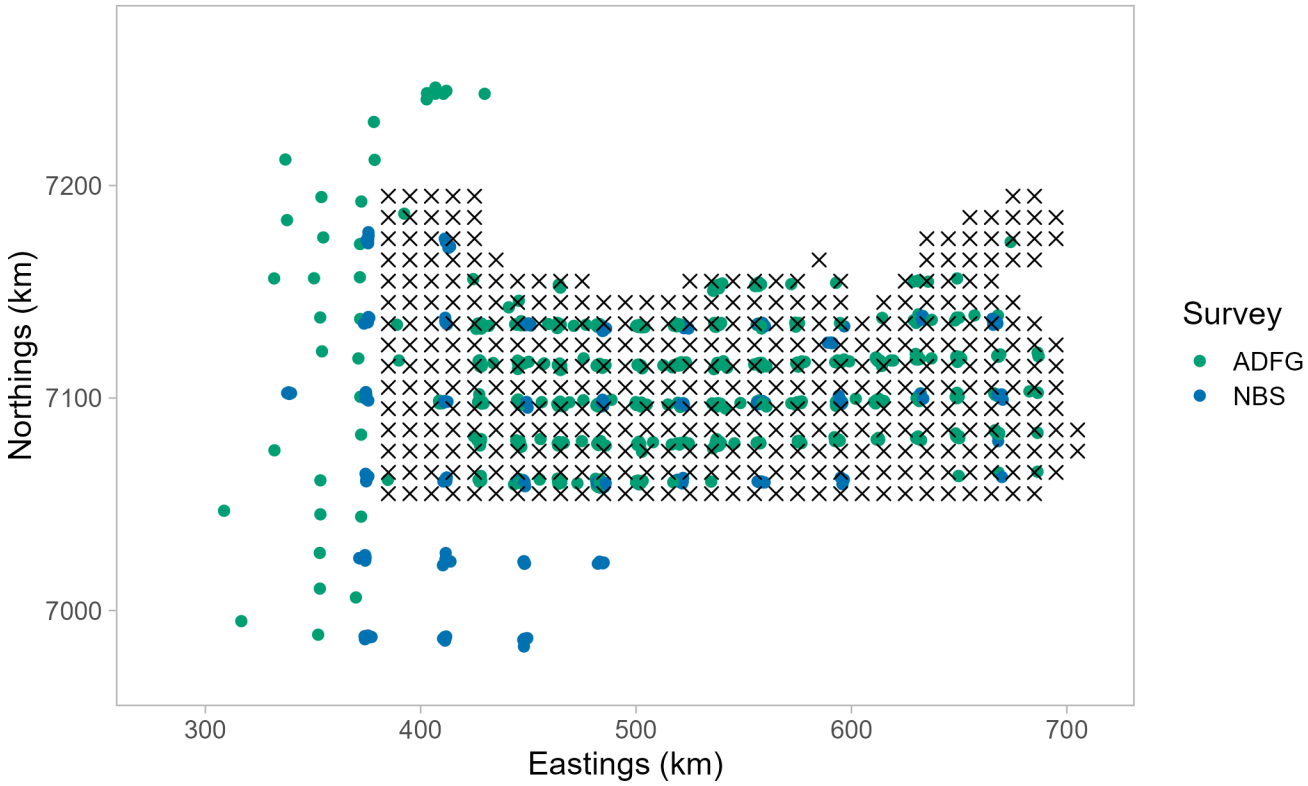


Figure 9: Smaller Norton Sound prediction grid used for red king crab spatial abundance predictions. Prediction grid spatial resolution is 10 km$^2$ and the grid does not include land. Survey data from all years of the ADF&G and NOAA NBS trawl surveys are shown for comparison.

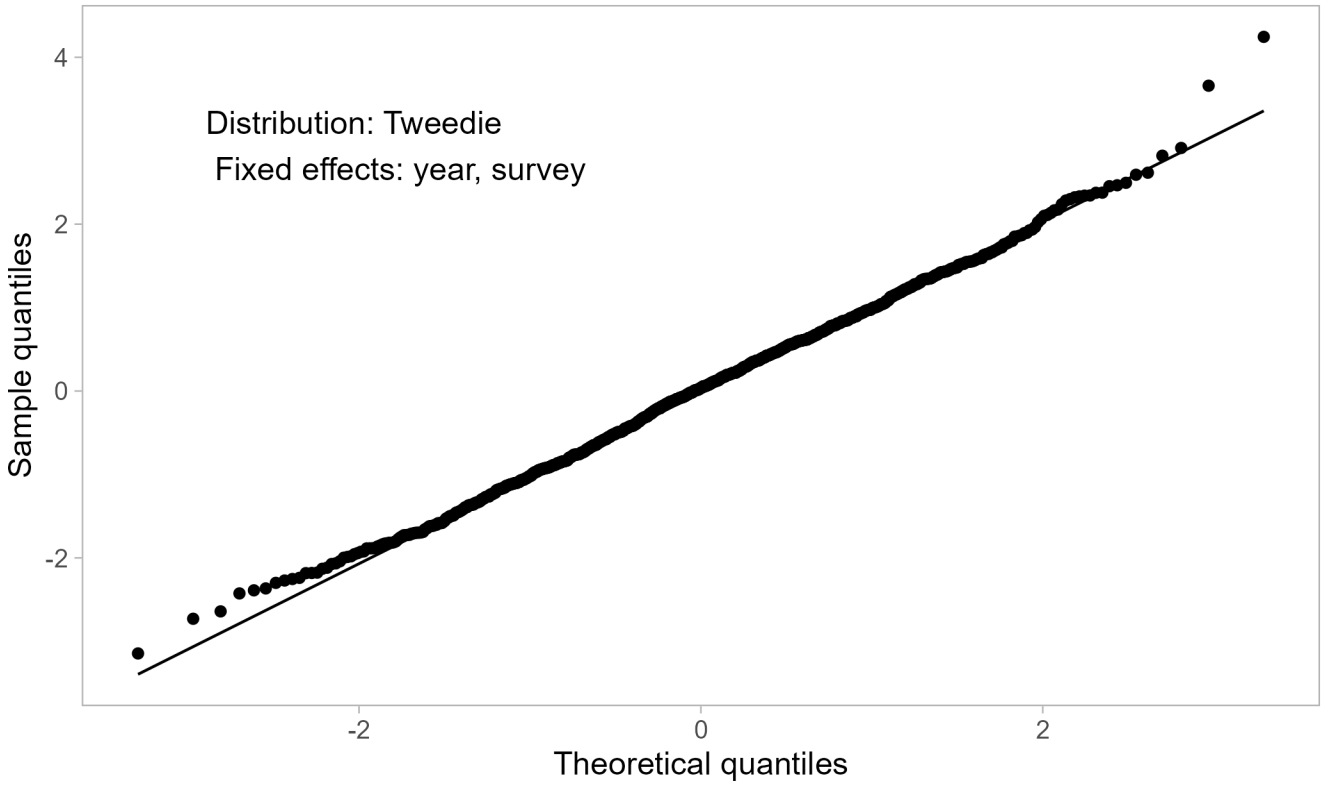


Figure 10: Quantile-quantile plot using MCMC-based randomized-quantile residuals for the model using the Tweedie distribution and year and survey fixed effects.

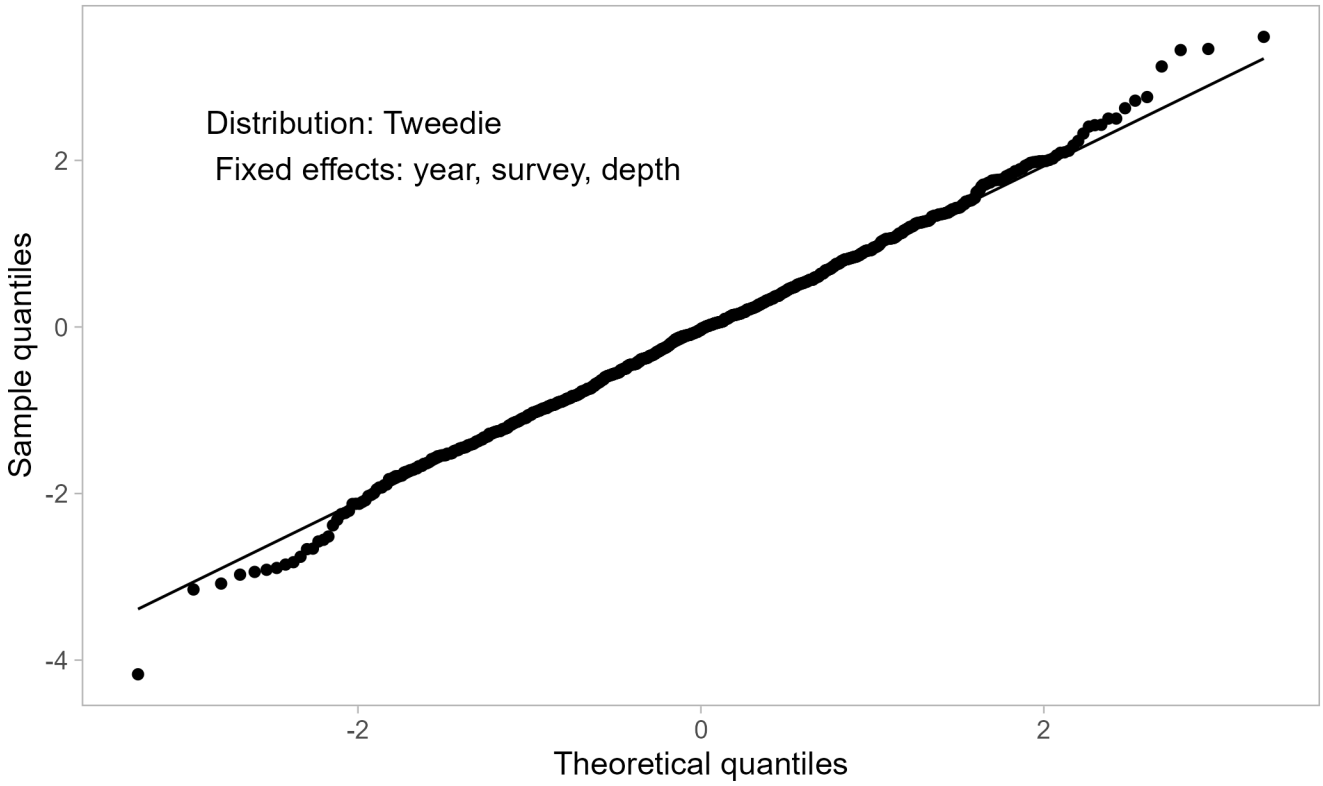


Figure 11: Quantile-quantile plot using MCMC-based randomized-quantile residuals for the model using the Tweedie distribution and year, survey, and depth fixed effects.

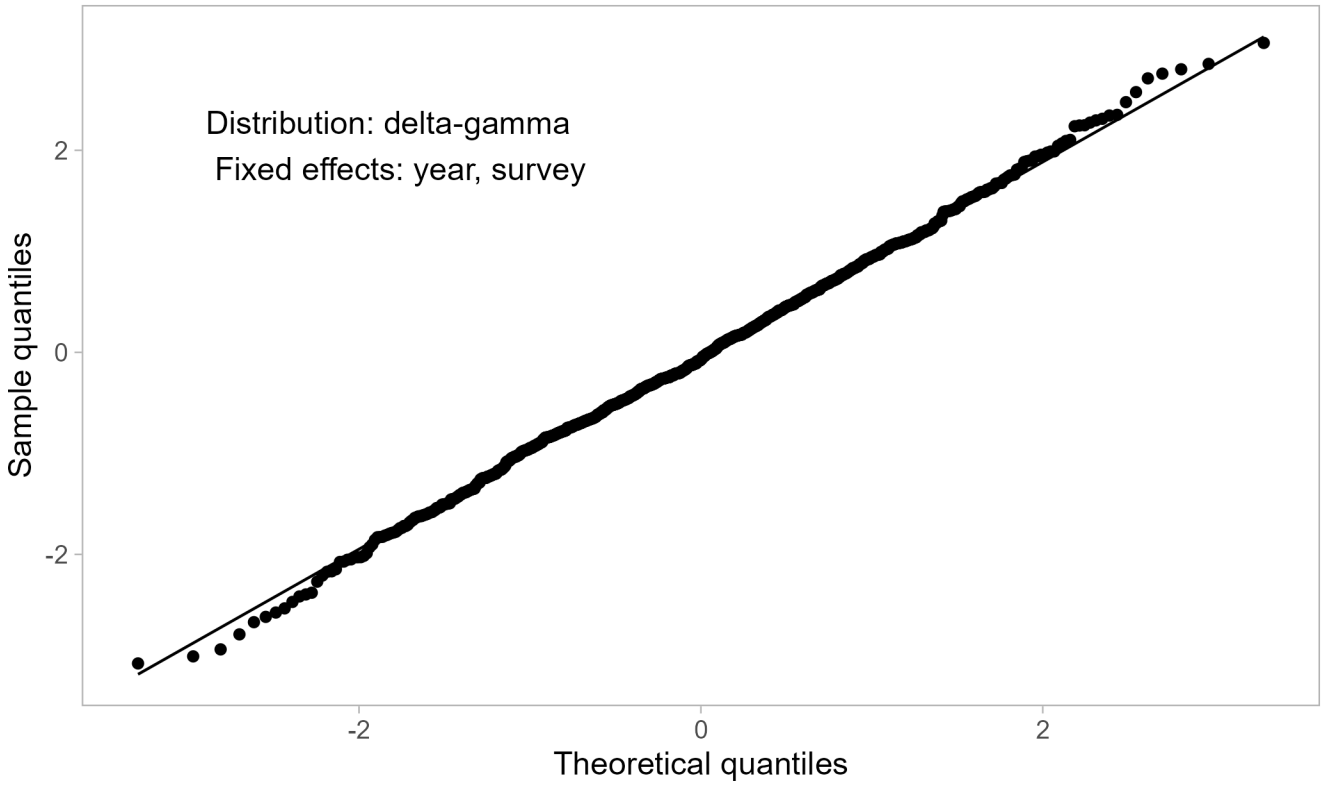


Figure 12: Quantile-quantile plot using MCMC-based randomized-quantile residuals for the model using the delta gamma distribution and year and survey fixed effects.

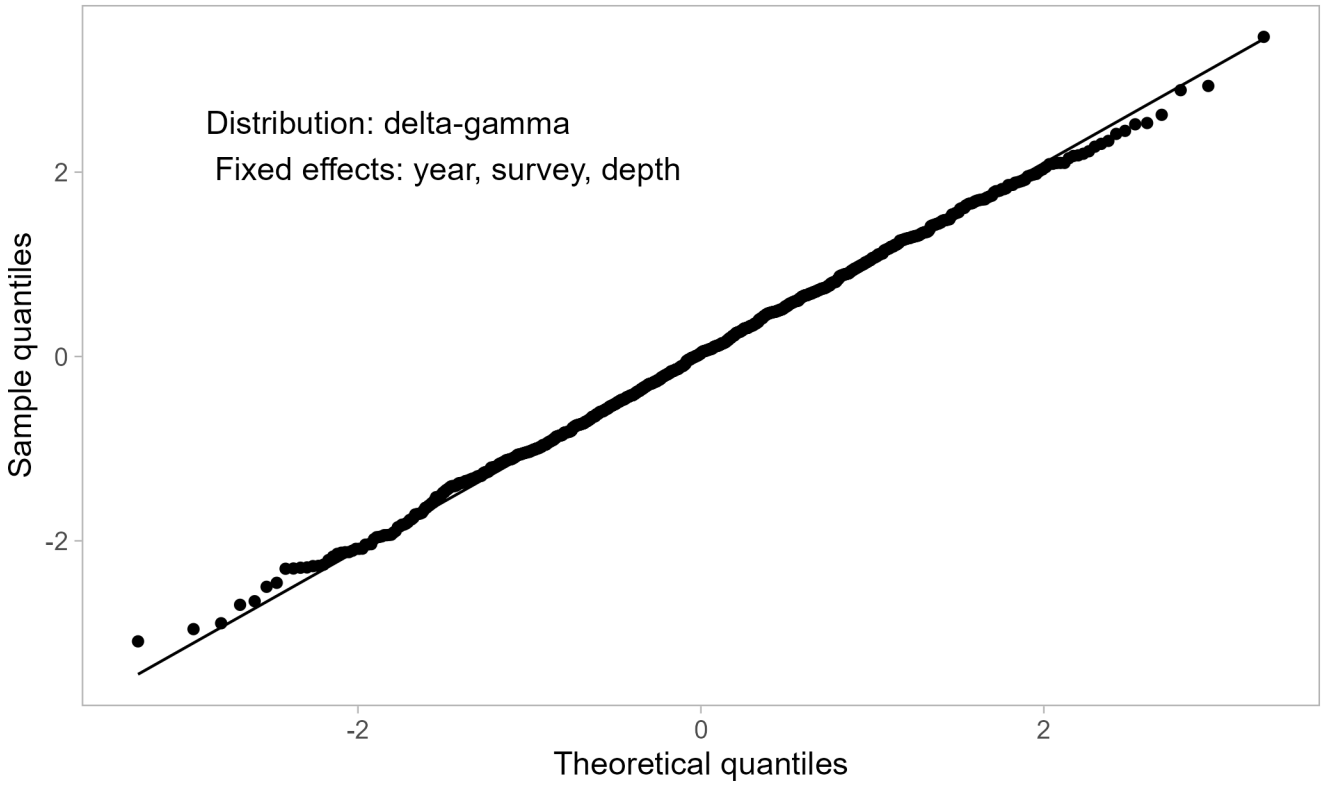


Figure 13: Quantile-quantile plot using MCMC-based randomized-quantile residuals for the model using the delta gamma distribution and year, survey, and depth fixed effects.

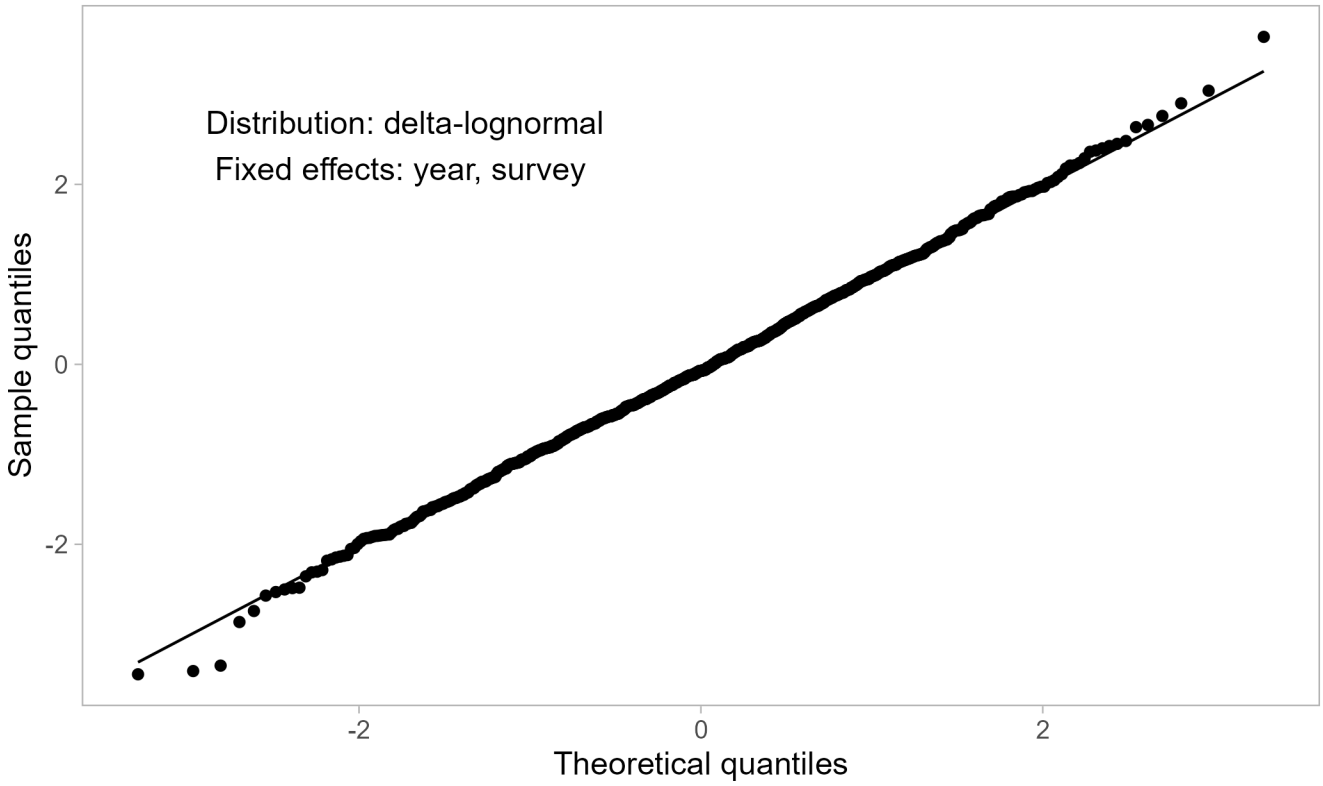


Figure 14: Quantile-quantile plot using MCMC-based randomized-quantile residuals for the model using the delta lognormal distribution and year and survey fixed effects.

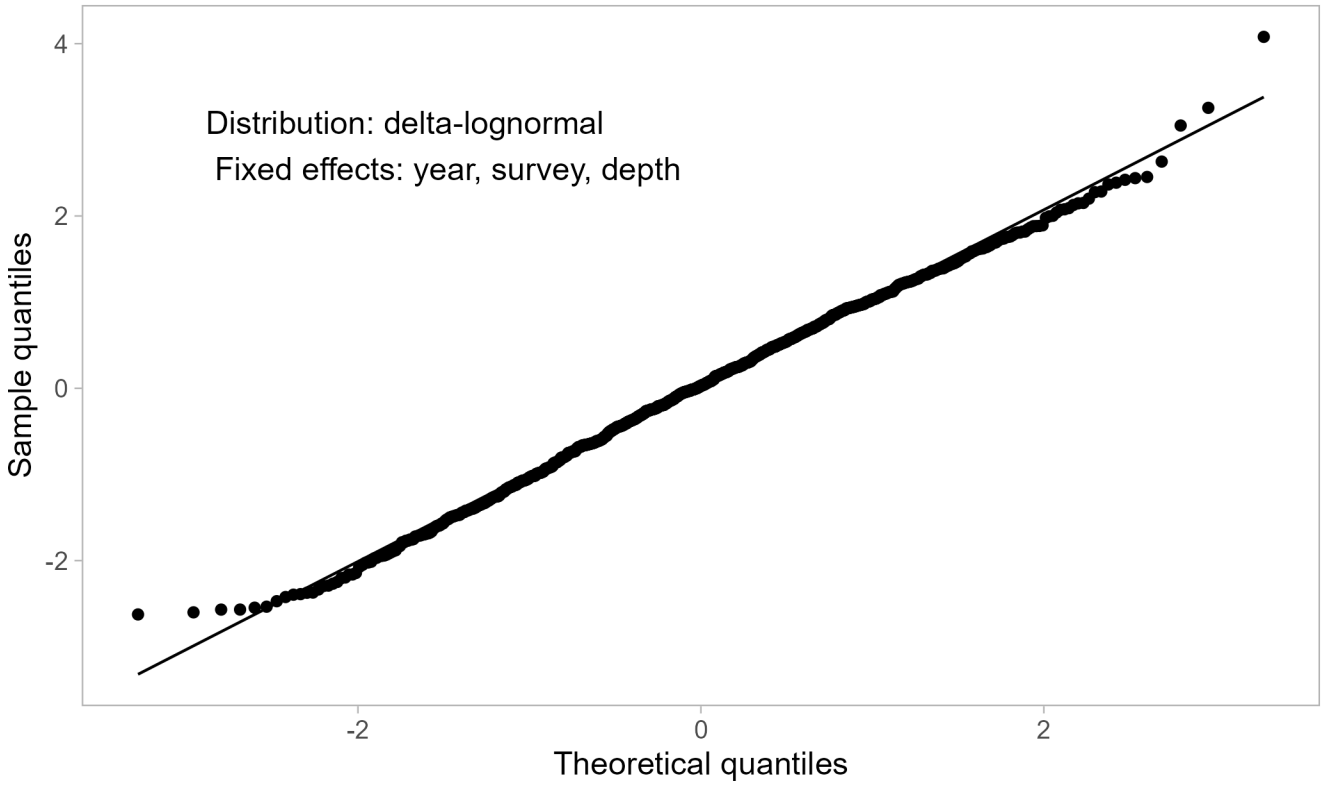


Figure 15: Quantile-quantile plot using MCMC-based randomized-quantile residuals for the model using the delta lognormal distribution and year, survey, and depth fixed effects.

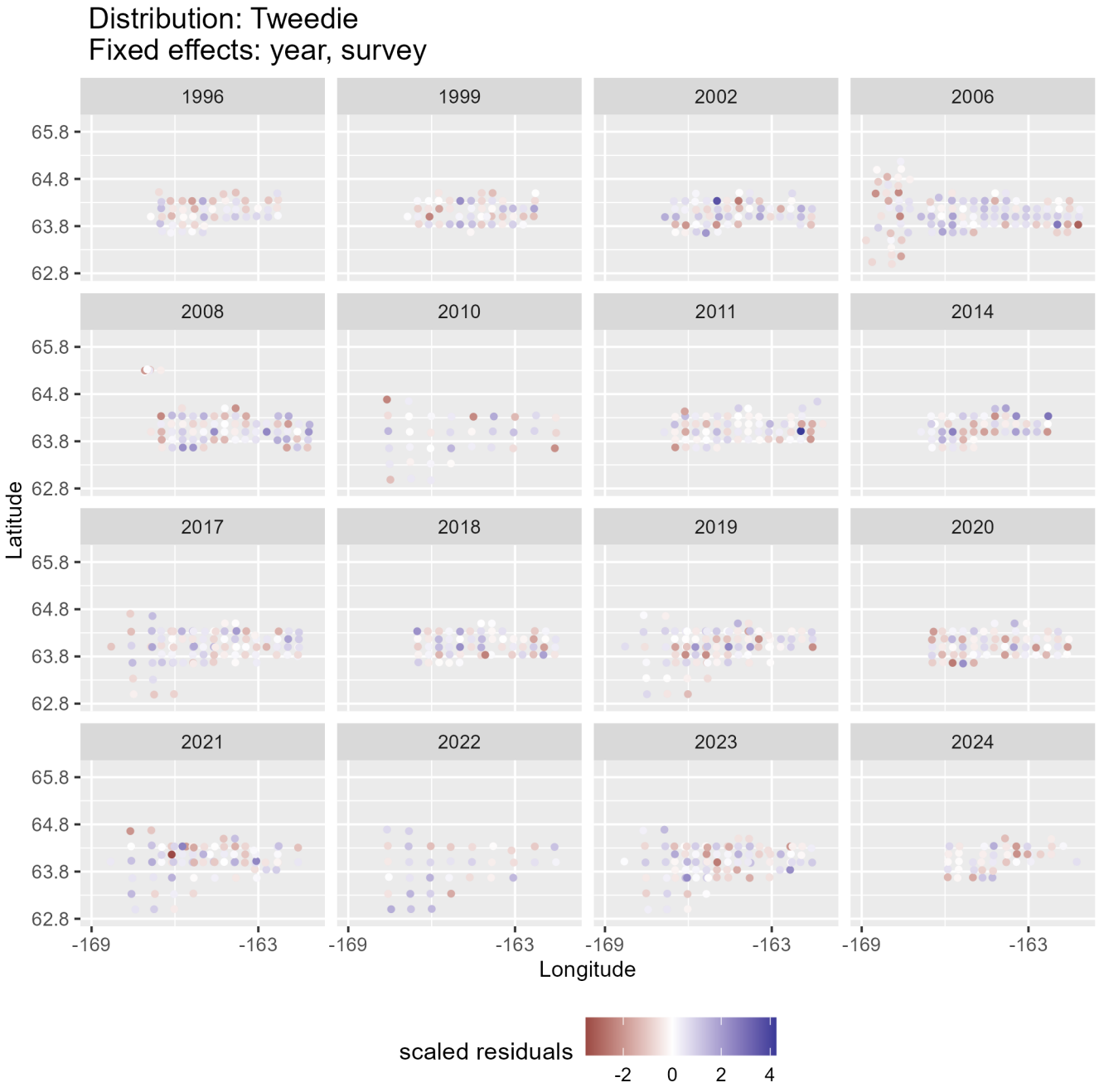


Figure 16: Spatial distribution of MCMC-based randomized-quantile residuals for the model using the Tweedie distribution with year and survey identity fixed effects.

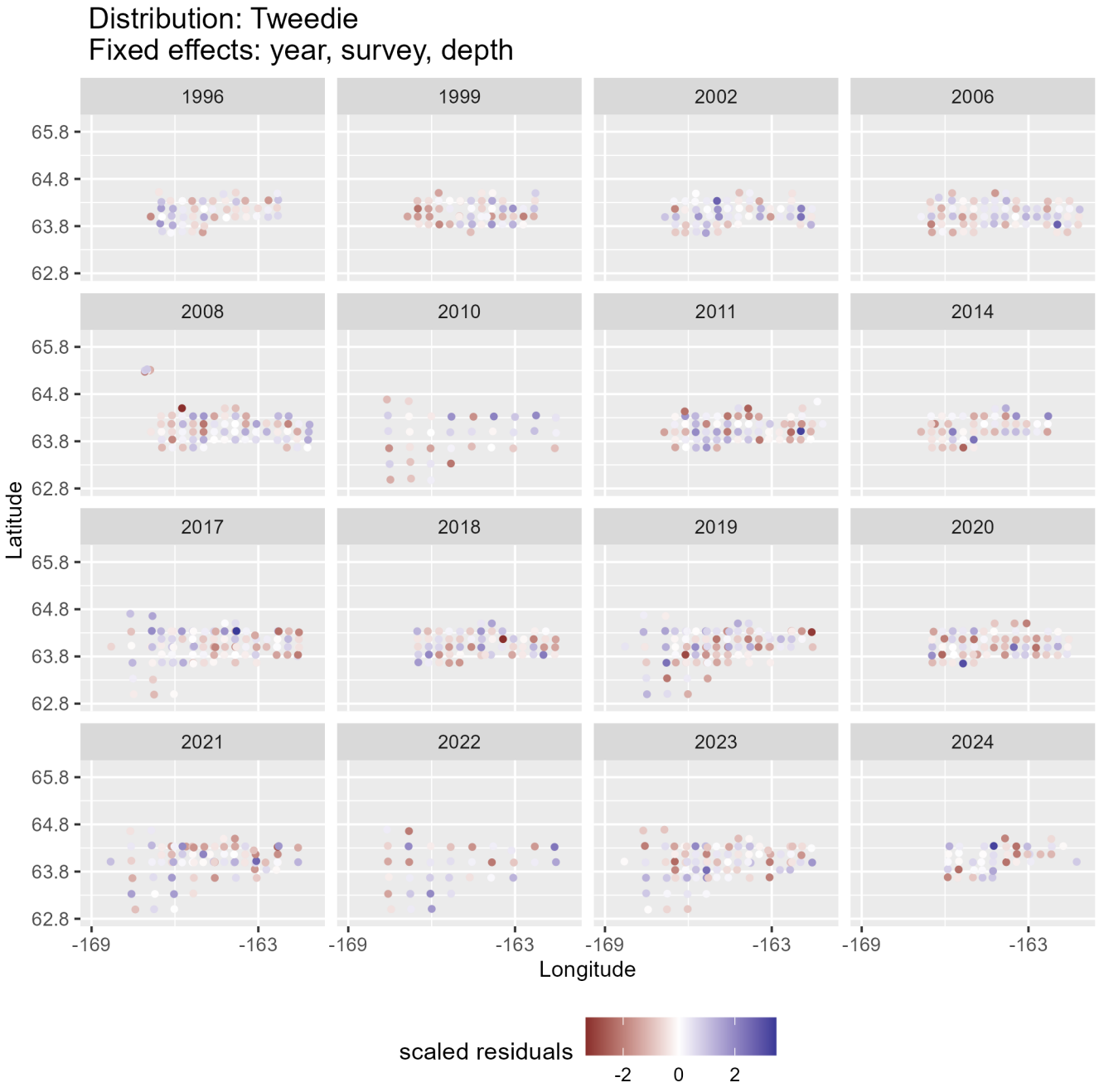


Figure 17: Spatial distribution of MCMC-based randomized-quantile residuals for the model using the Tweedie distribution with year, survey identity, and depth fixed effects.

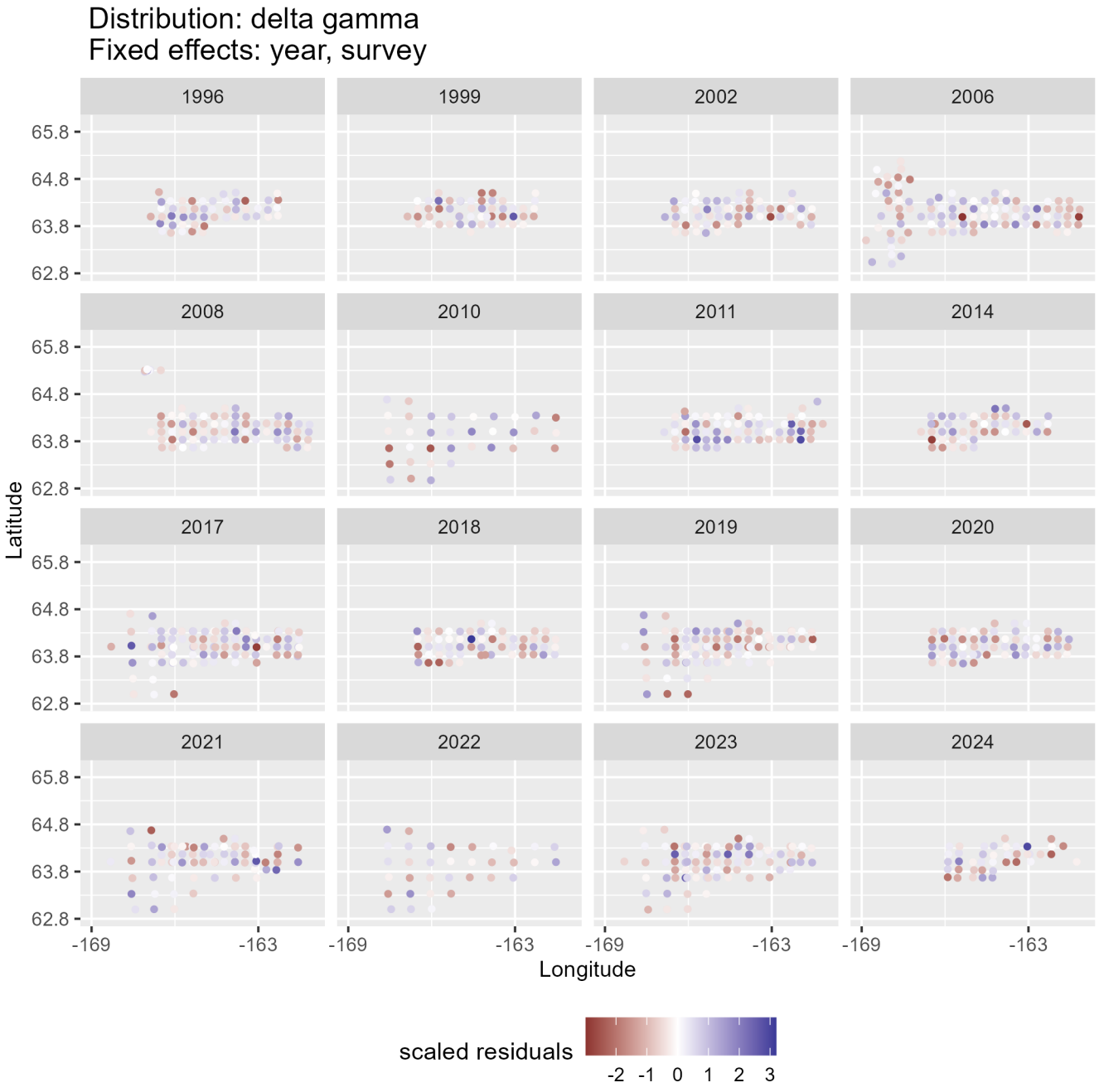


Figure 18: Spatial distribution of MCMC-based randomized-quantile residuals for the model using the delta gamma distribution with year and survey identity fixed effects.

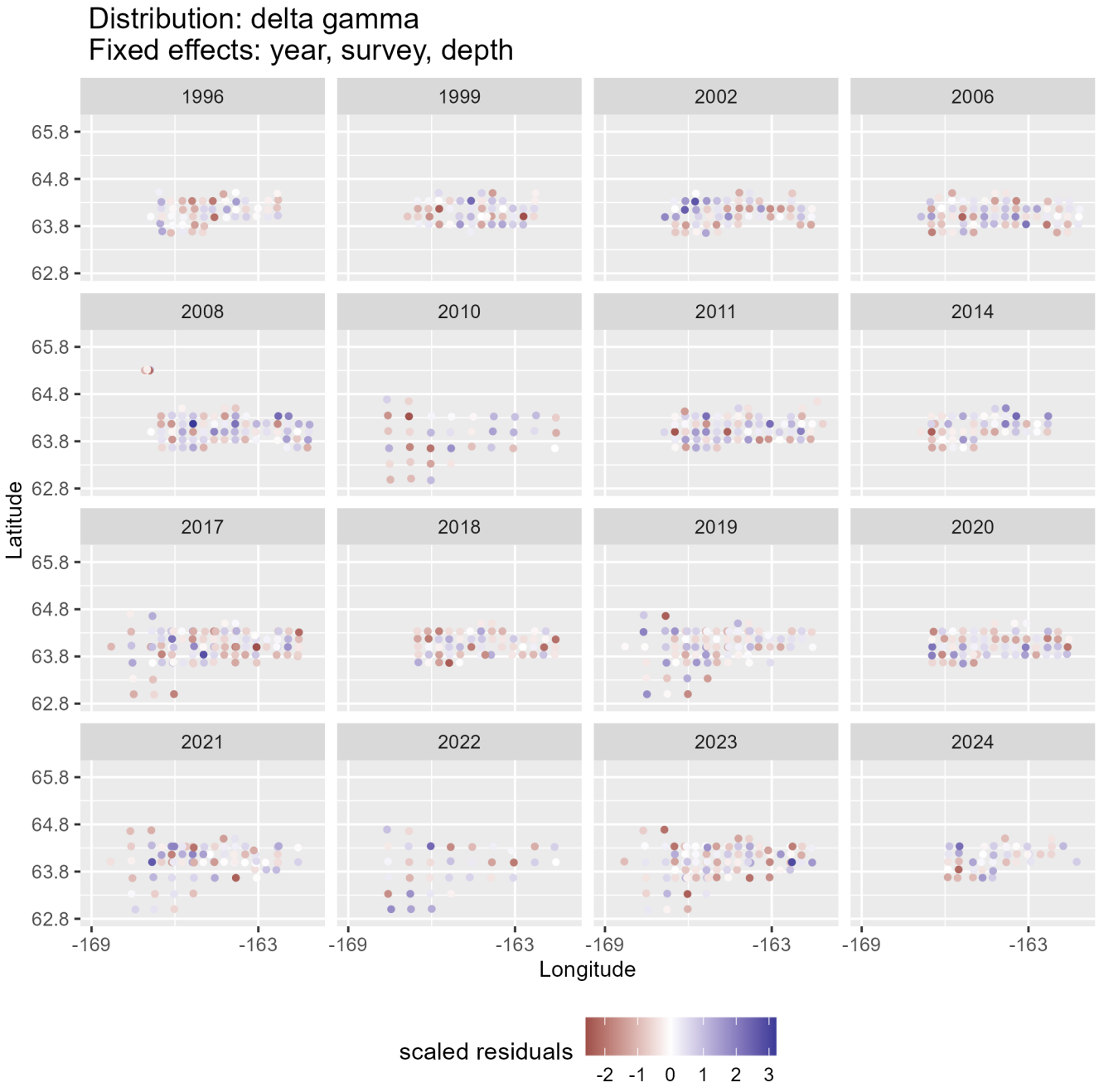


Figure 19: Spatial distribution of MCMC-based randomized-quantile residuals for the model using the delta gamma distribution with year, survey identity, and depth fixed effects.

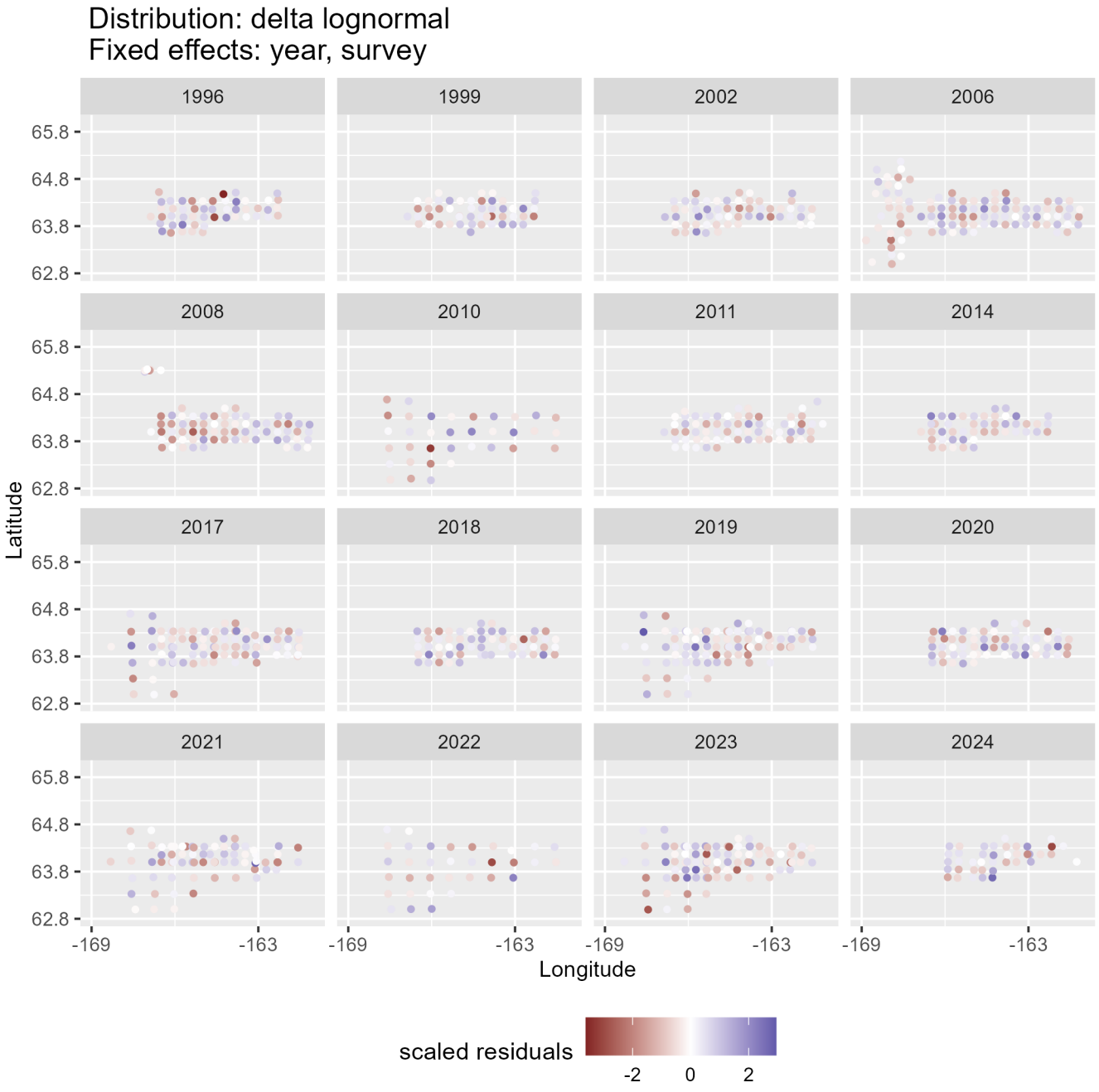


Figure 20: Spatial distribution of MCMC-based randomized-quantile residuals for the model using the delta lognormal distribution with year and survey identity fixed effects.

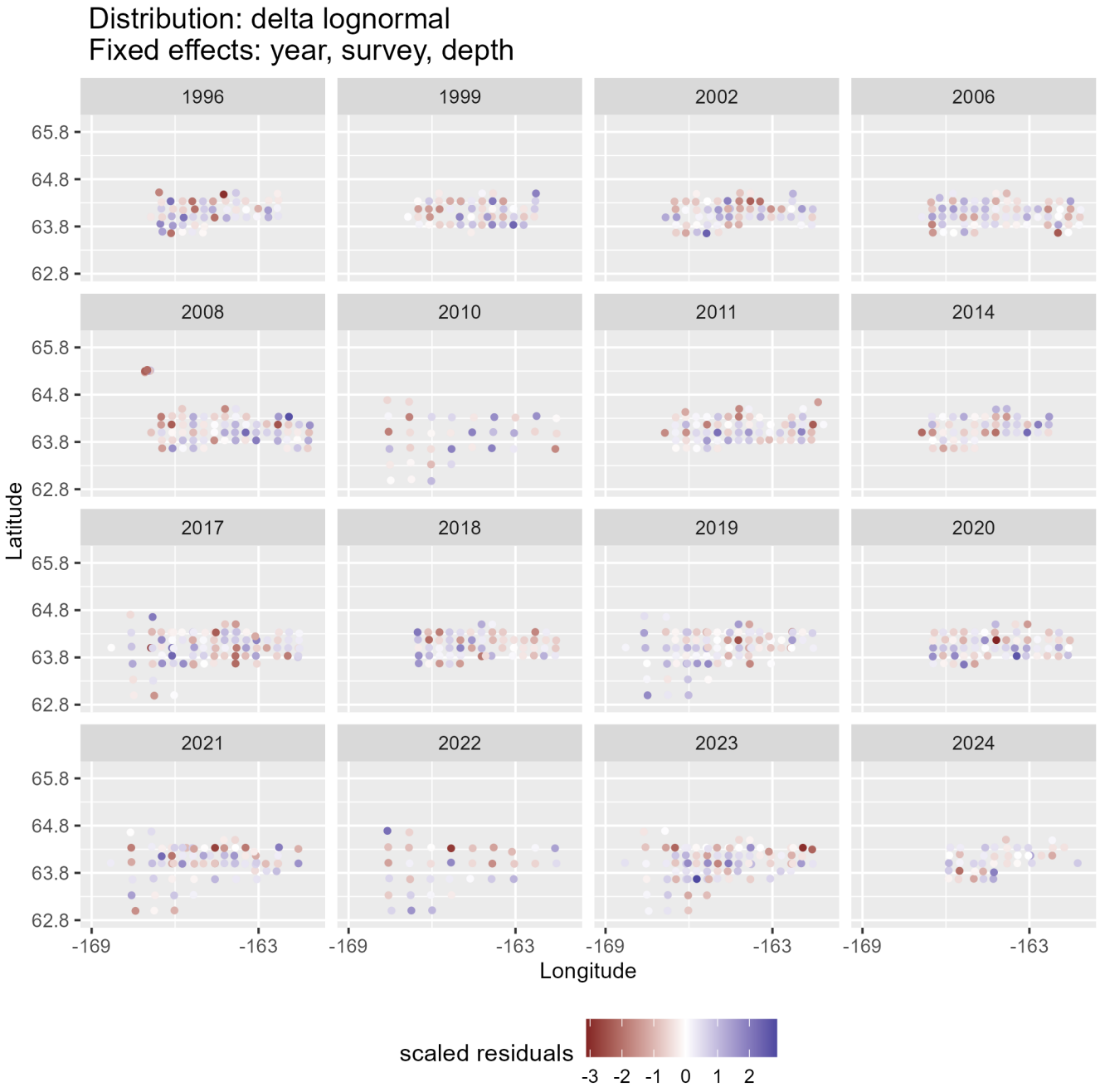


Figure 21: Spatial distribution of MCMC-based randomized-quantile residuals for the model using the delta lognormal distribution with year, survey identity, and depth fixed effects.

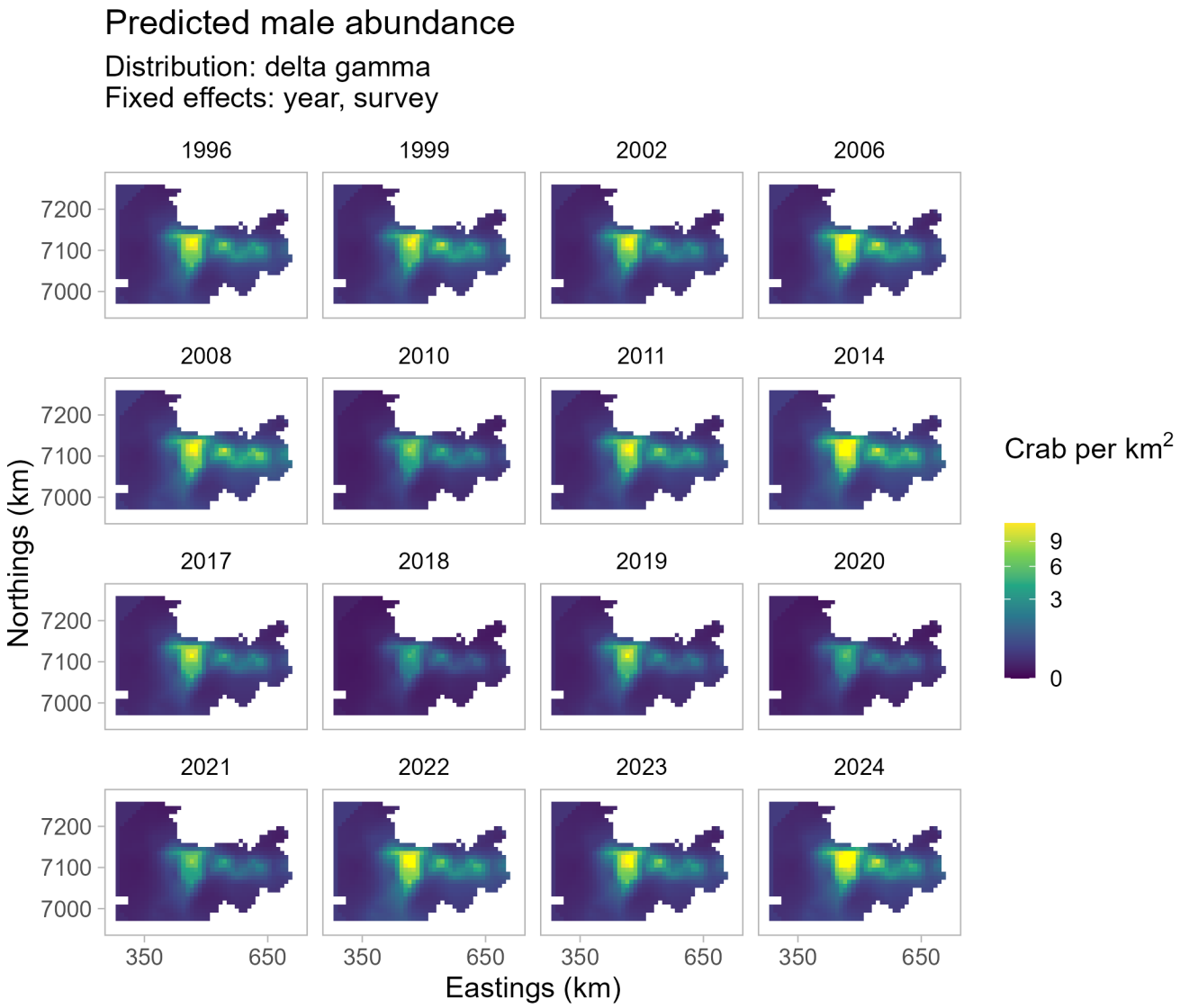


Figure 22: Predicted abundance over the larger prediction grid of Norton Sound red king crab males $\geq$ 64 mm in carapace length by year from the model using the delta gamma distribution with year and survey identity fixed effects.

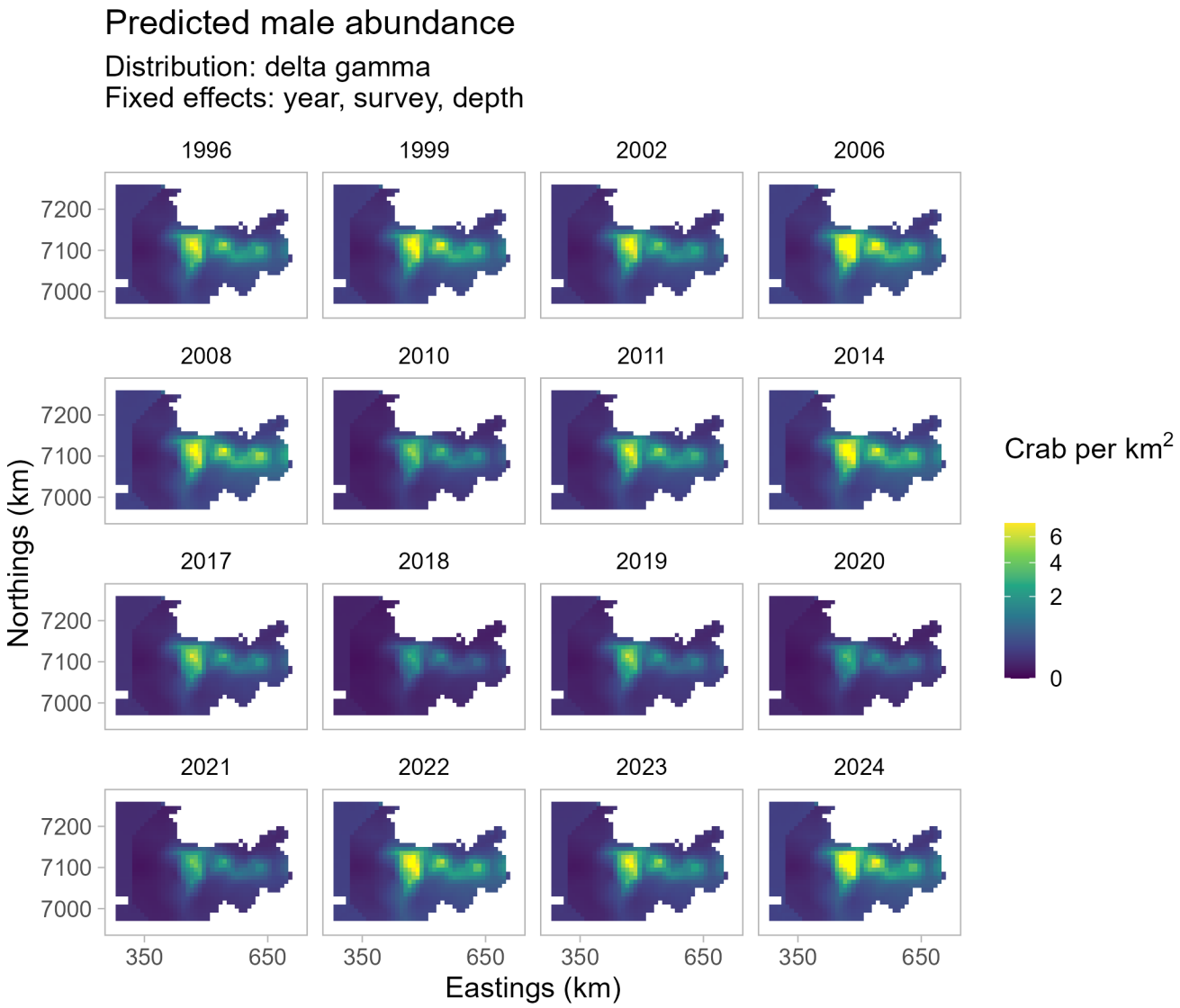


Figure 23: Predicted abundance over the larger prediction grid of Norton Sound red king crab males $\geq$ 64 mm in carapace length by year from the model using the delta gamma distribution with year, survey identity, and depth fixed effects.

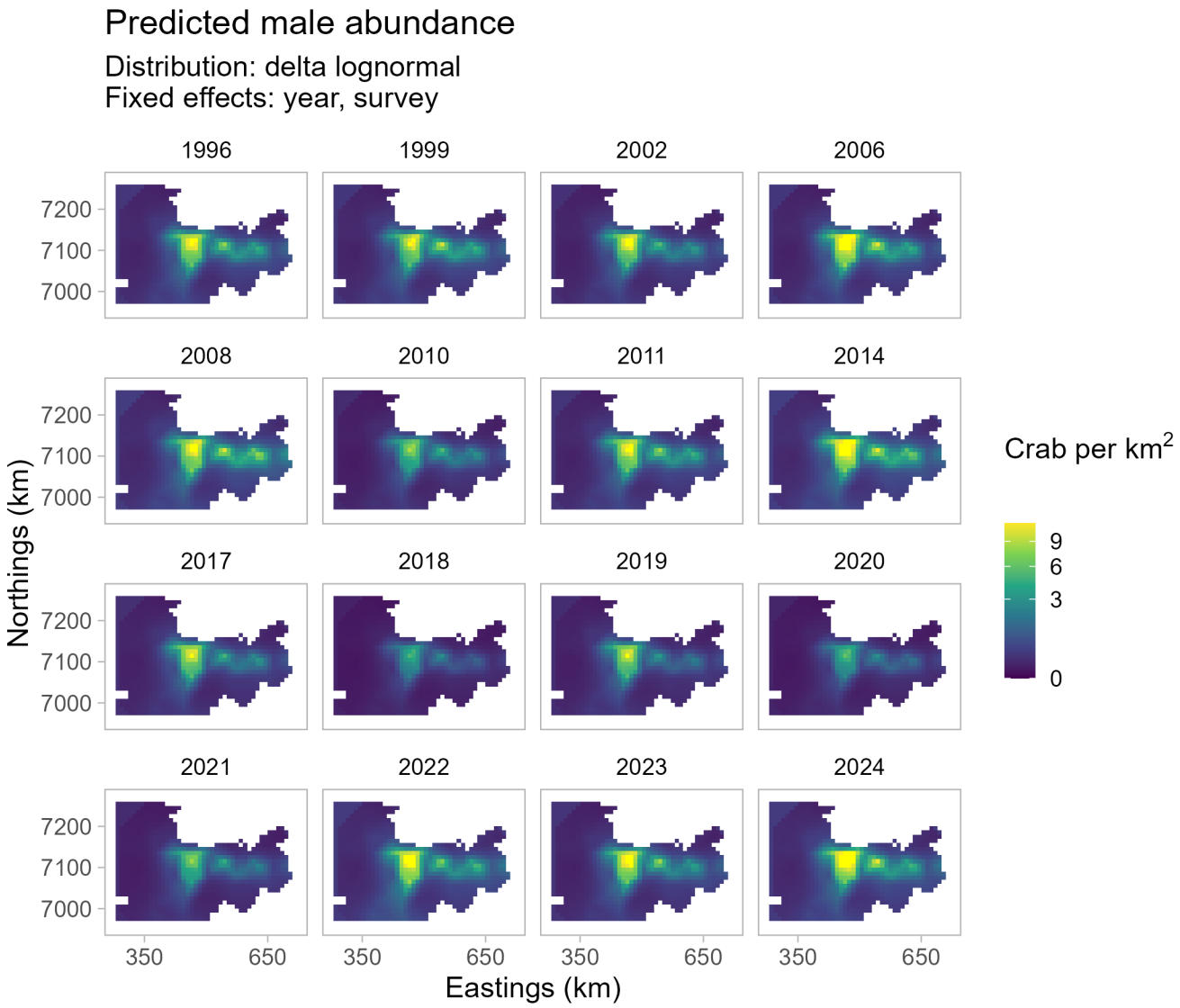


Figure 24: Predicted abundance over the larger prediction grid of Norton Sound red king crab males $\geq$ 64 mm in carapace length by year from the model using the delta lognormal distribution with year and survey identity fixed effects.

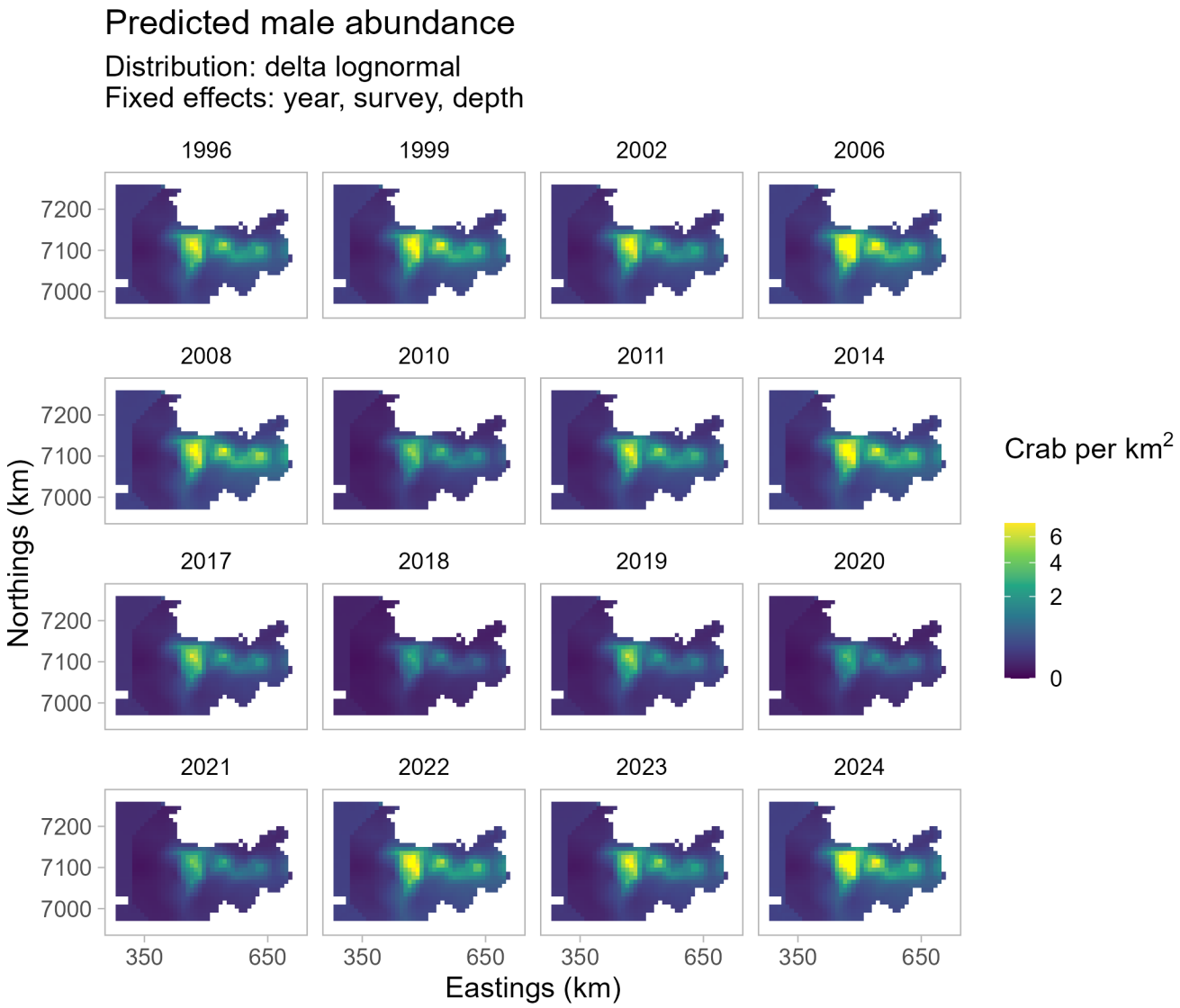


Figure 25: Predicted abundance over the larger prediction grid of Norton Sound red king crab males $\geq$ 64 mm in carapace length by year from the model using the delta lognormal distribution with year, survey identity, and depth fixed effects.

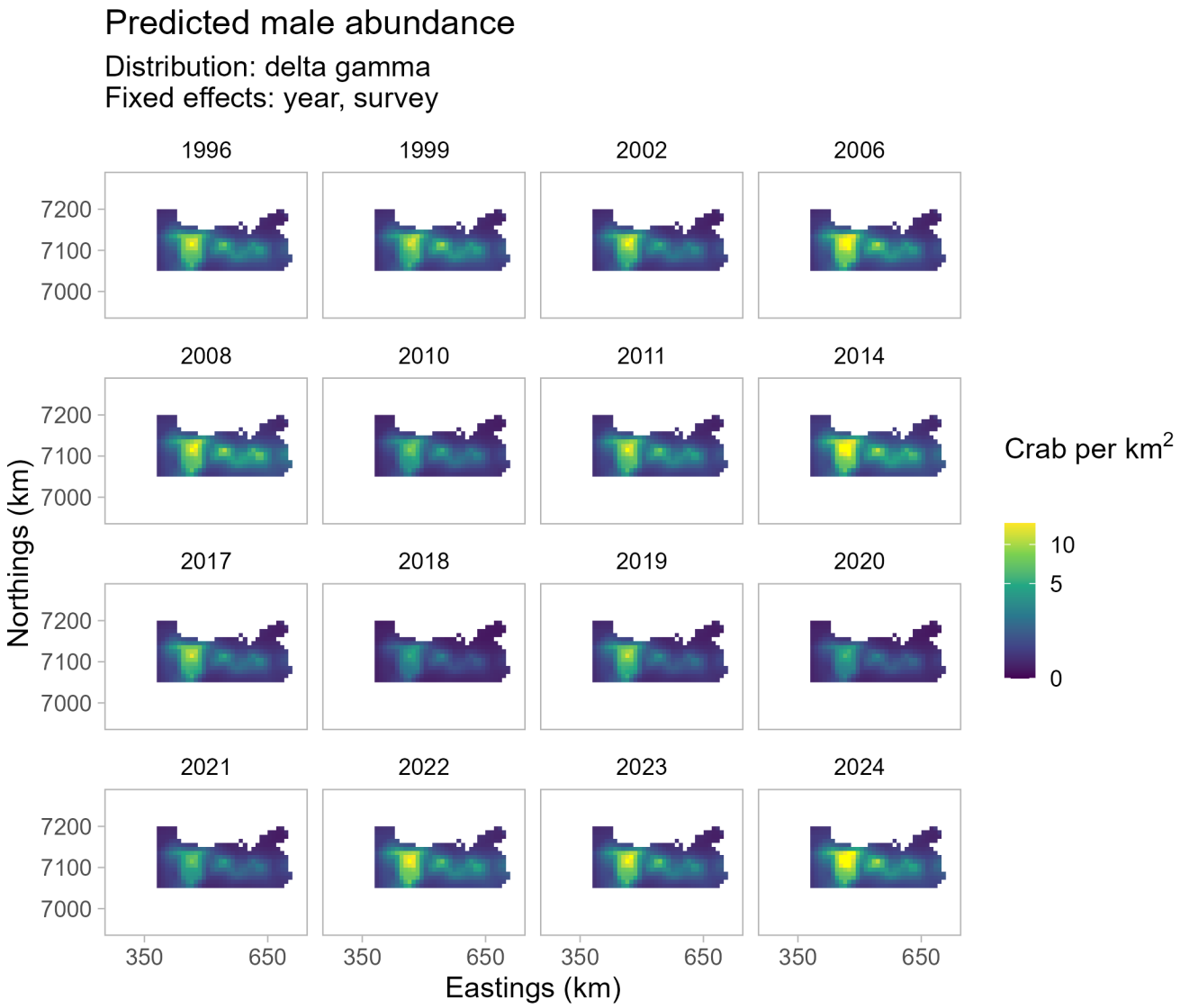


Figure 26: Predicted abundance over the smaller prediction grid of Norton Sound red king crab males $\geq$ 64 mm in carapace length by year from the model using the delta gamma distribution with year and survey identity fixed effects.

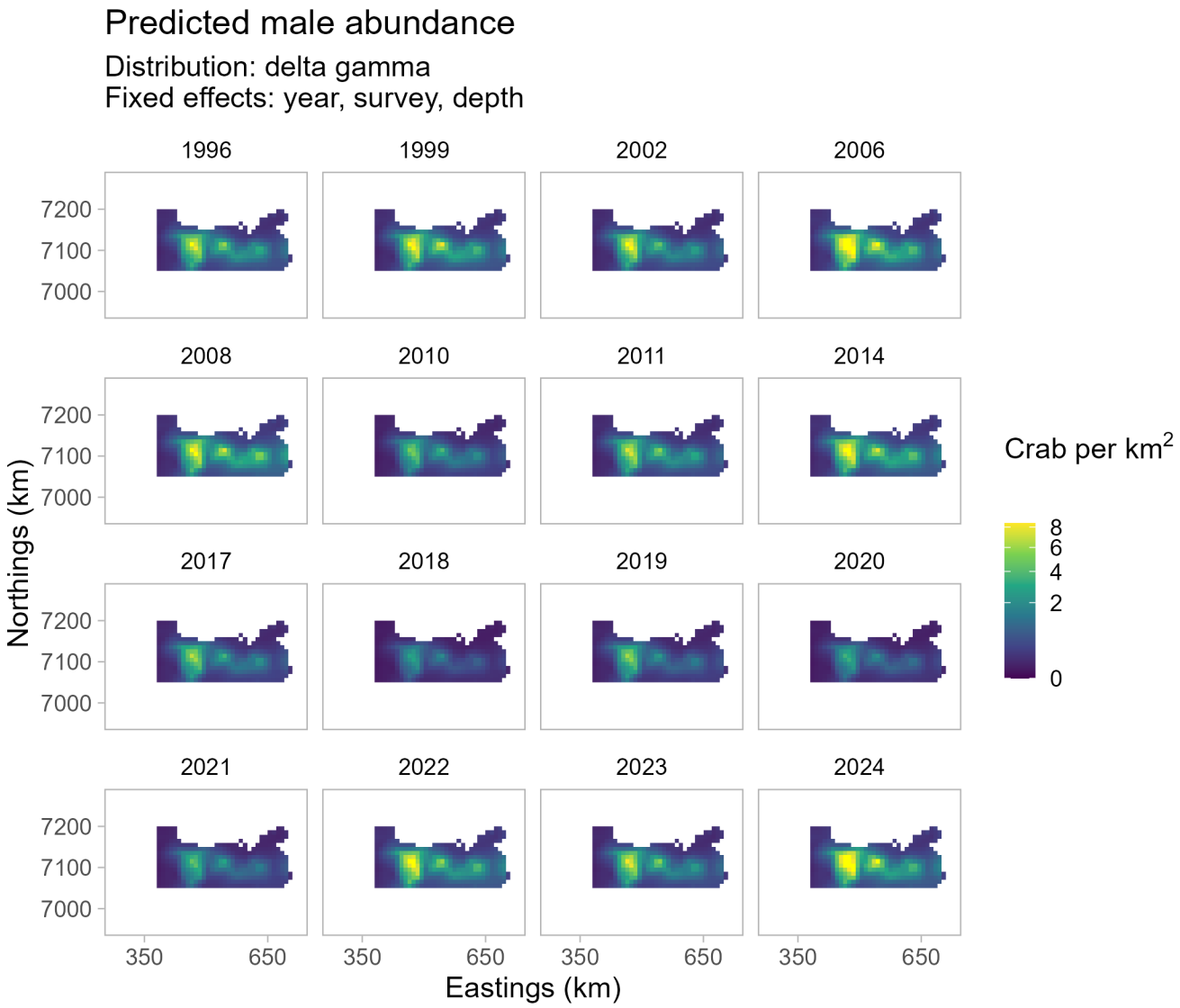


Figure 27: Predicted abundance over the smaller prediction grid of Norton Sound red king crab males $\geq$ 64 mm in carapace length by year from the model using the delta gamma distribution with year, survey identity, and depth fixed effects.

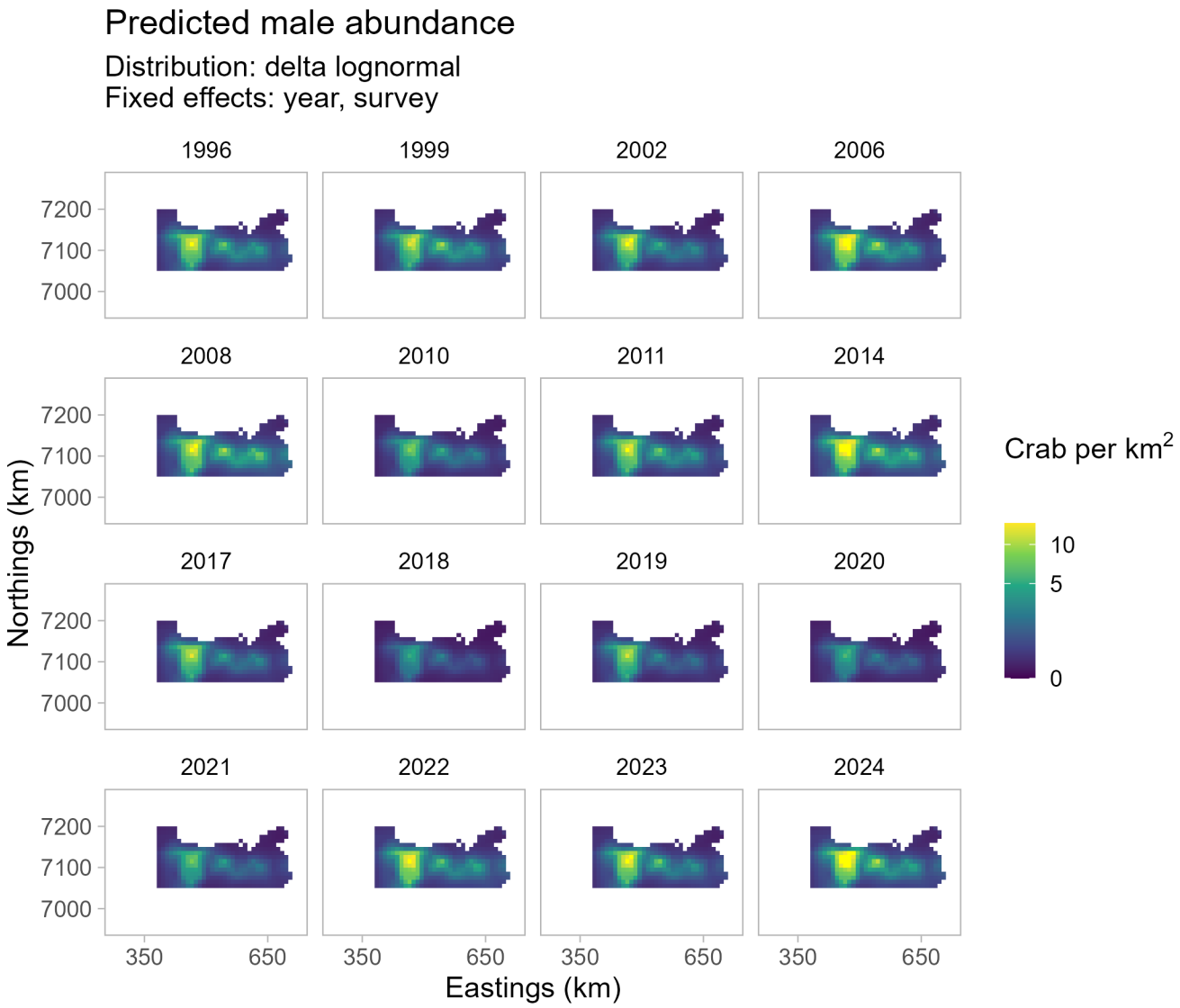


Figure 28: Predicted abundance over the smaller prediction grid of Norton Sound red king crab males $\geq$ 64 mm in carapace length by year from the model using the delta lognormal distribution with year and survey identity fixed effects.

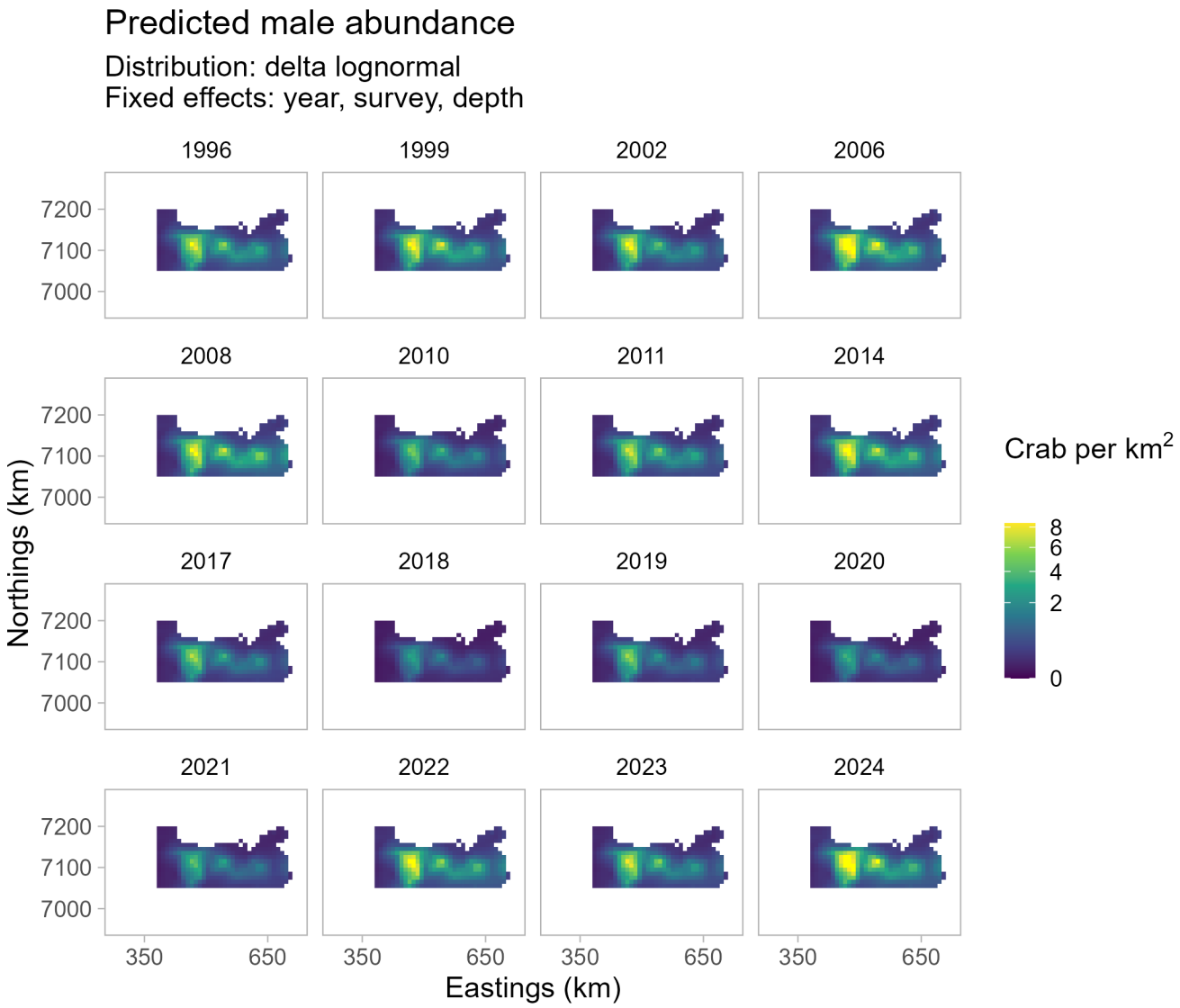


Figure 29: Predicted abundance over the smaller prediction grid of Norton Sound red king crab males $\geq$ 64 mm in carapace length by year from the model using the delta lognormal distribution with year, survey identity, and depth fixed effects.

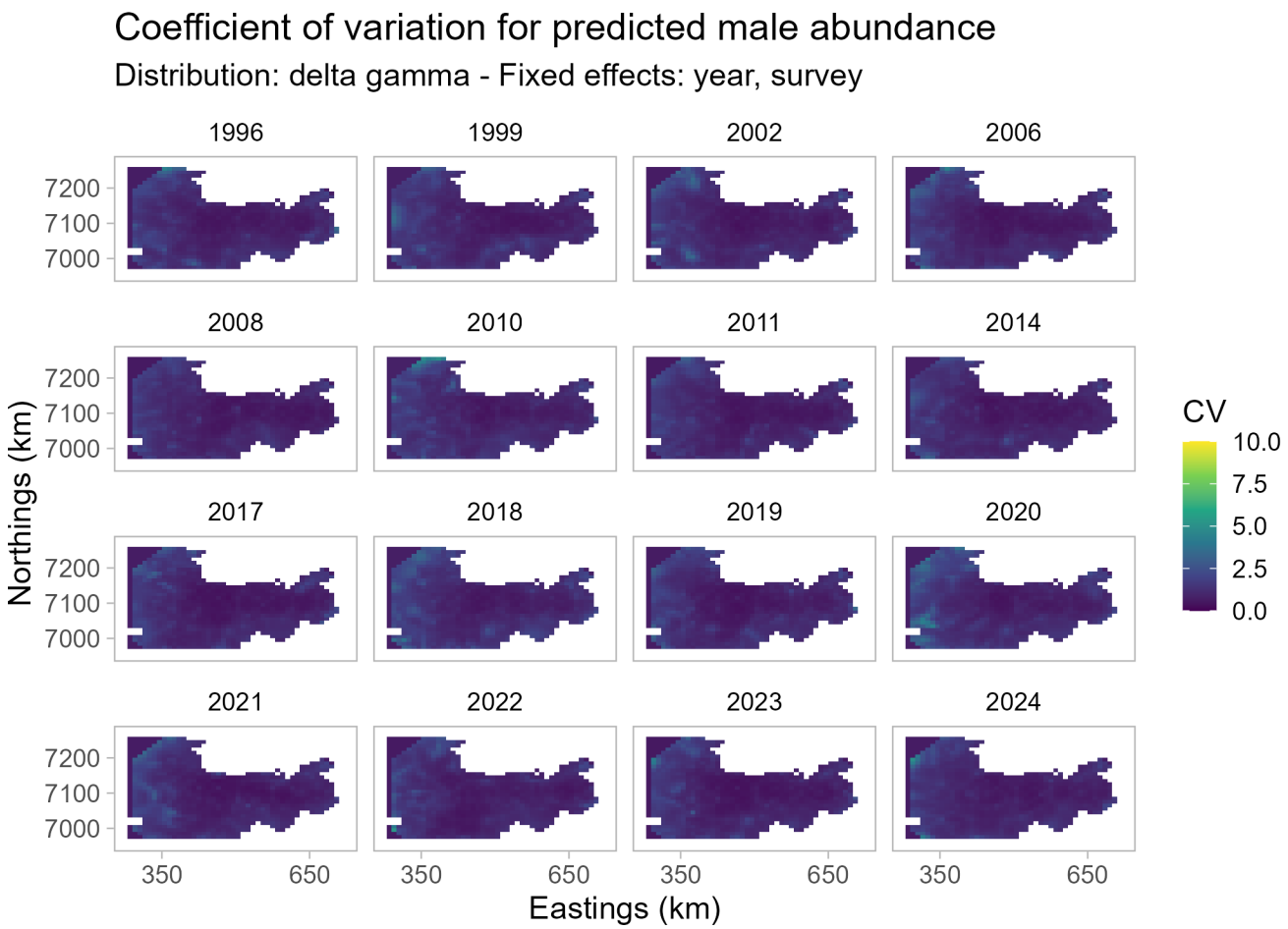


Figure 30: Coefficient of variation (CV) for predicted abundance over the larger prediction grid of Norton Sound red king crab males $\geq$ 64 mm in carapace length by year from the model using the delta gamma distribution with year and survey identity fixed effects.

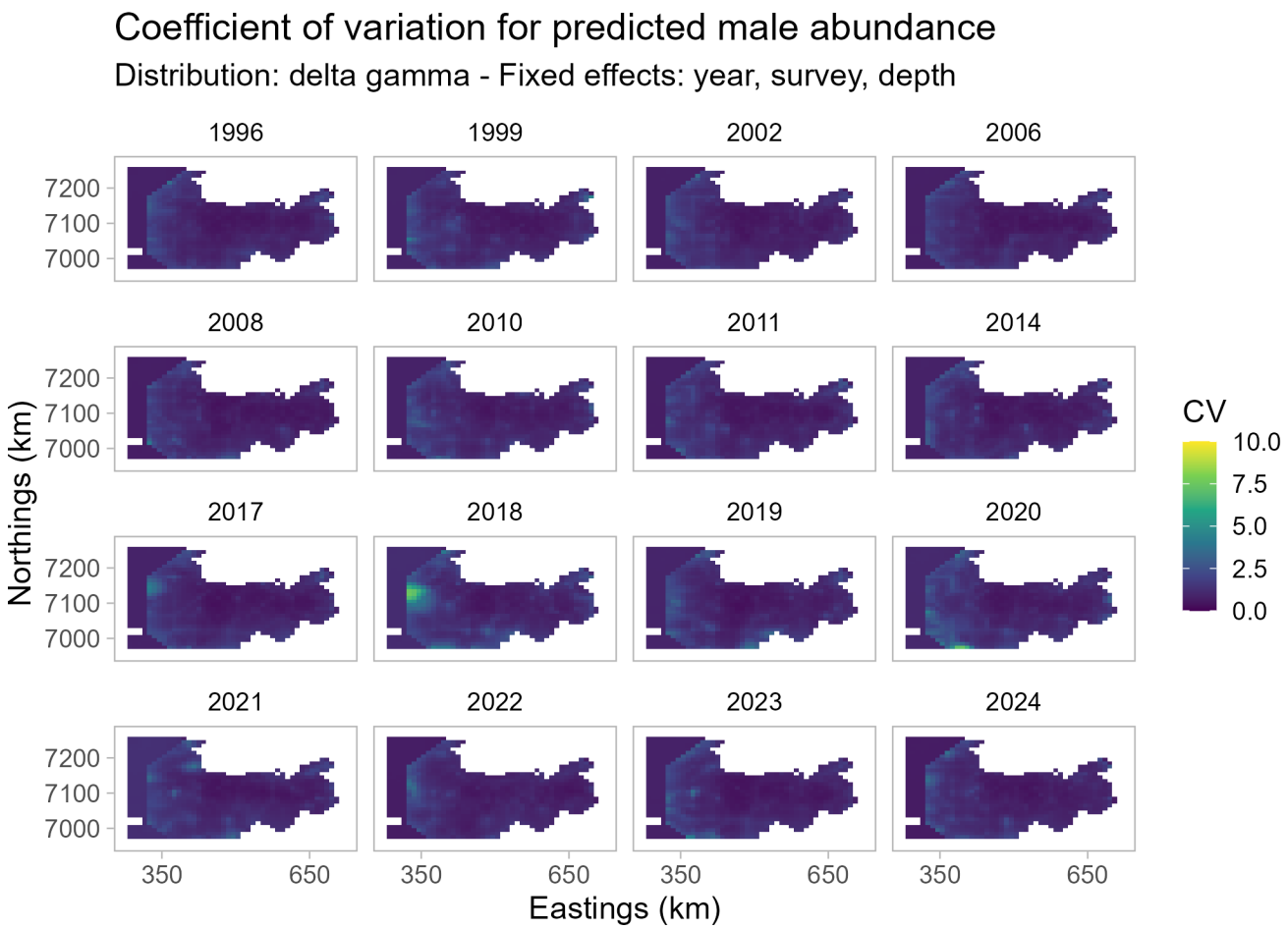


Figure 31: Coefficient of variation (CV) for predicted abundance over the larger prediction grid of Norton Sound red king crab males $\geq$ 64 mm in carapace length by year from the model using the delta gamma distribution with year, survey identity, and depth fixed effects.

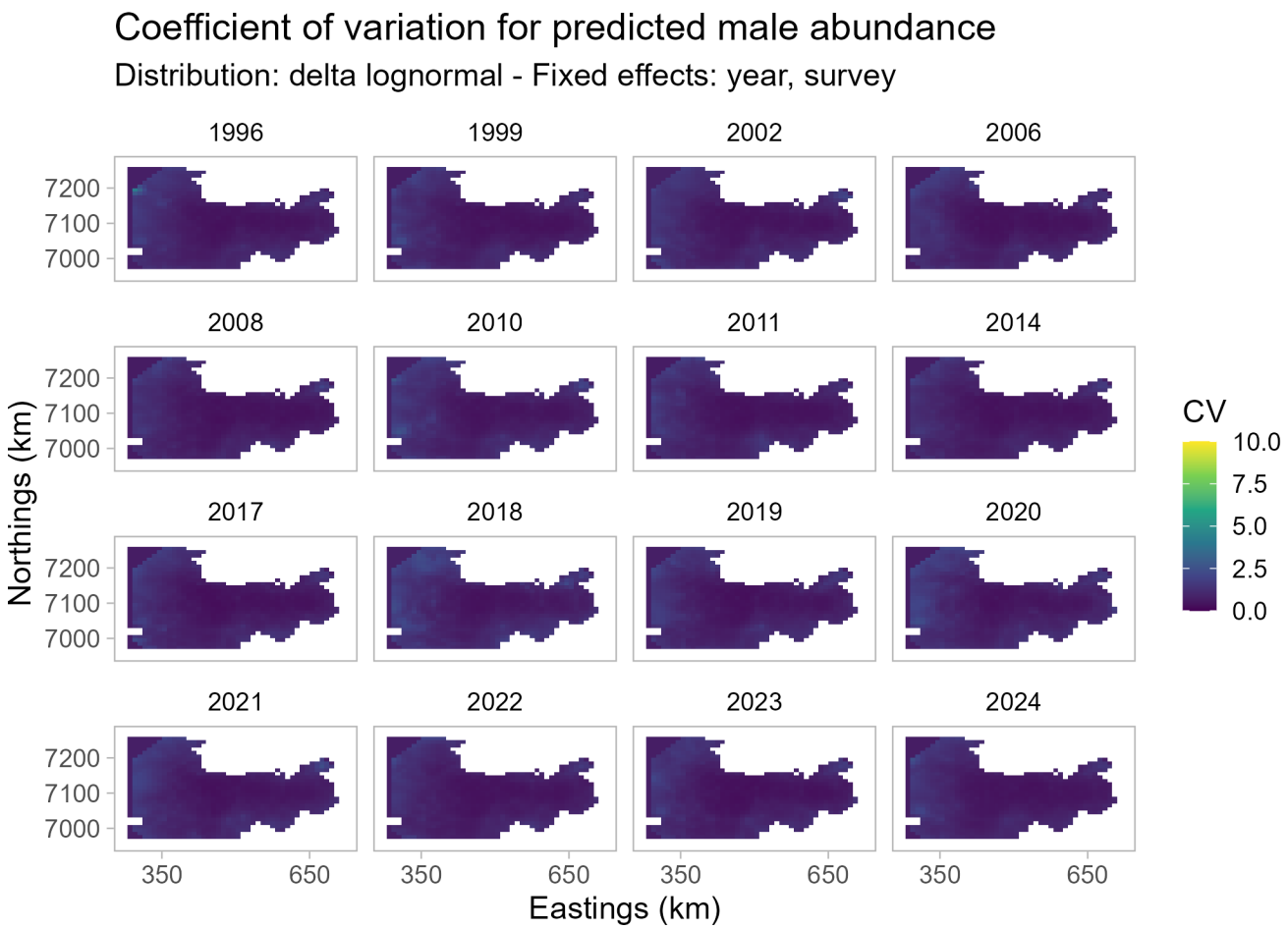


Figure 32: Coefficient of variation (CV) for predicted abundance over the larger prediction grid of Norton Sound red king crab males $\geq$ 64 mm in carapace length by year from the model using the delta lognormal distribution with year and survey identity fixed effects.

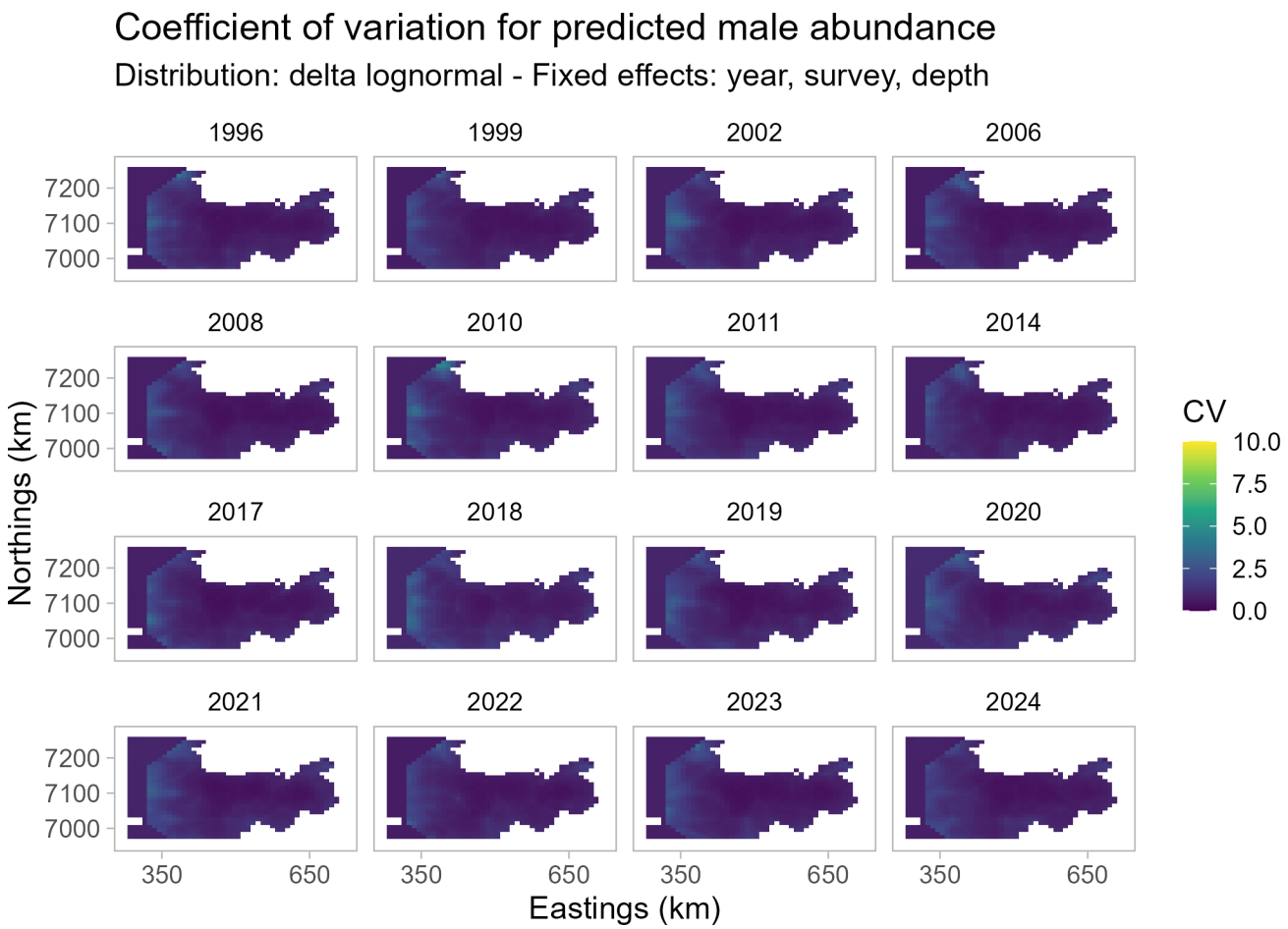


Figure 33: Coefficient of variation (CV) for predicted abundance over the larger prediction grid of Norton Sound red king crab males $\geq$ 64 mm in carapace length by year from the model using the delta lognormal distribution with year, survey identity, and depth fixed effects.

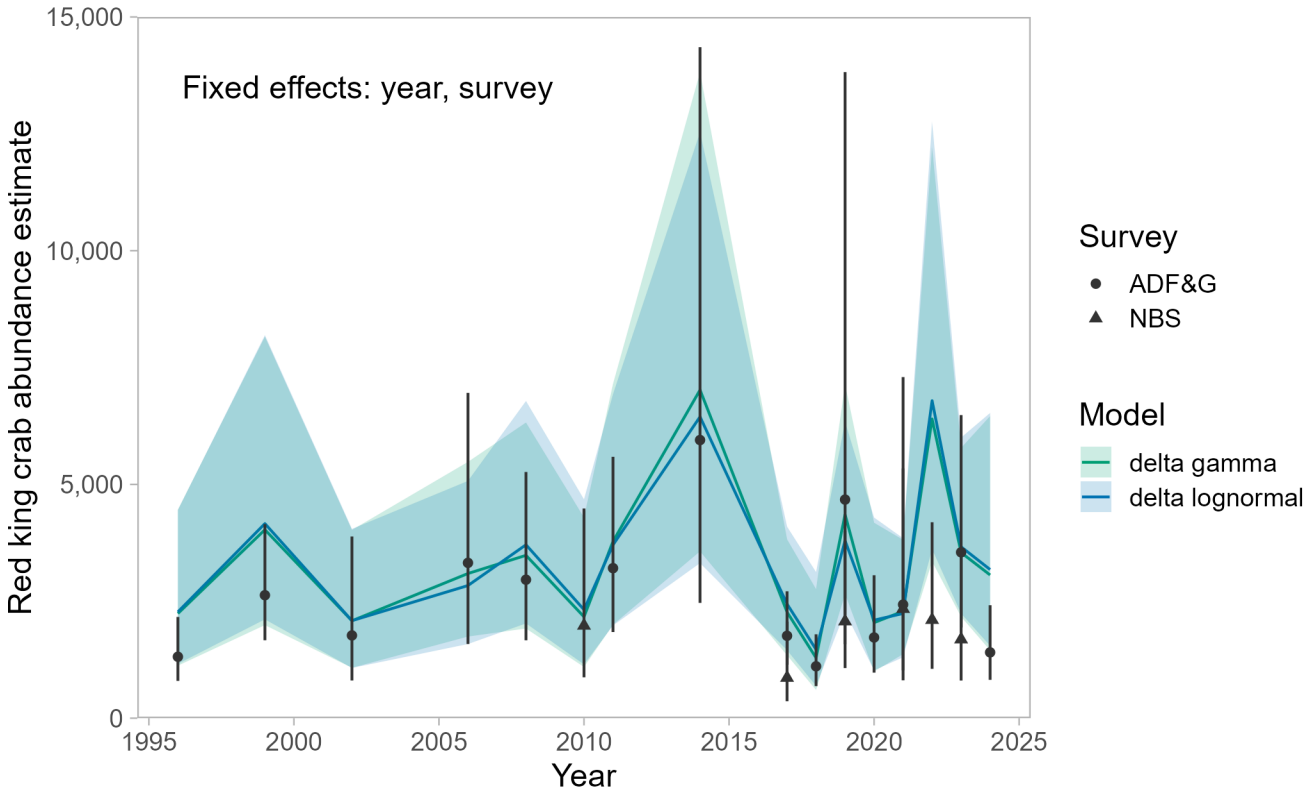


Figure 34: Estimated abundance (1000's of crab) using the larger prediction grid for male Norton Sound red king crab with carapace length $\geq$ 64 mm from models combining data from the ADF&G and NBS trawl surveys. Colored lines represent abundance ($\pm$95% CI) estimated using sdmTMB with either the delta gamma (green) or delta lognormal (blue) distribution. Year and survey identity were included as fixed effects. Black points represent design-based abundance ($\pm$95% CI) estimates currently used in the stock assessment model.

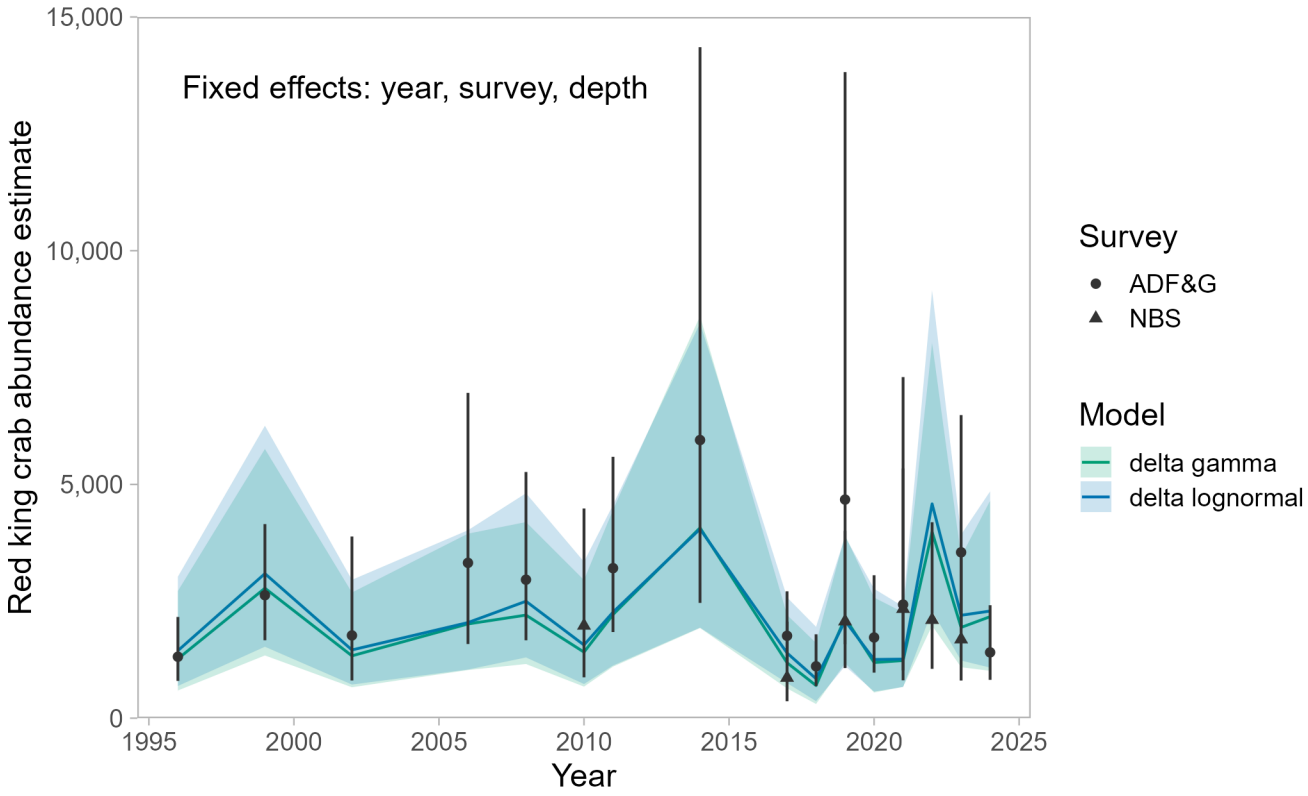


Figure 35: Estimated abundance (1000's of crab) using the larger prediction grid for male Norton Sound red king crab with carapace length $\geq$ 64 mm from models combining data from the ADF&G and NBS trawl surveys. Colored lines represent abundance ($\pm$95% CI) estimated using sdmTMB with either the delta gamma (green) or delta lognormal (blue) distribution. Year, survey identity, and depth were included as fixed effects. Black points represent design-based abundance ($\pm$95% CI) estimates currently used in the stock assessment model.

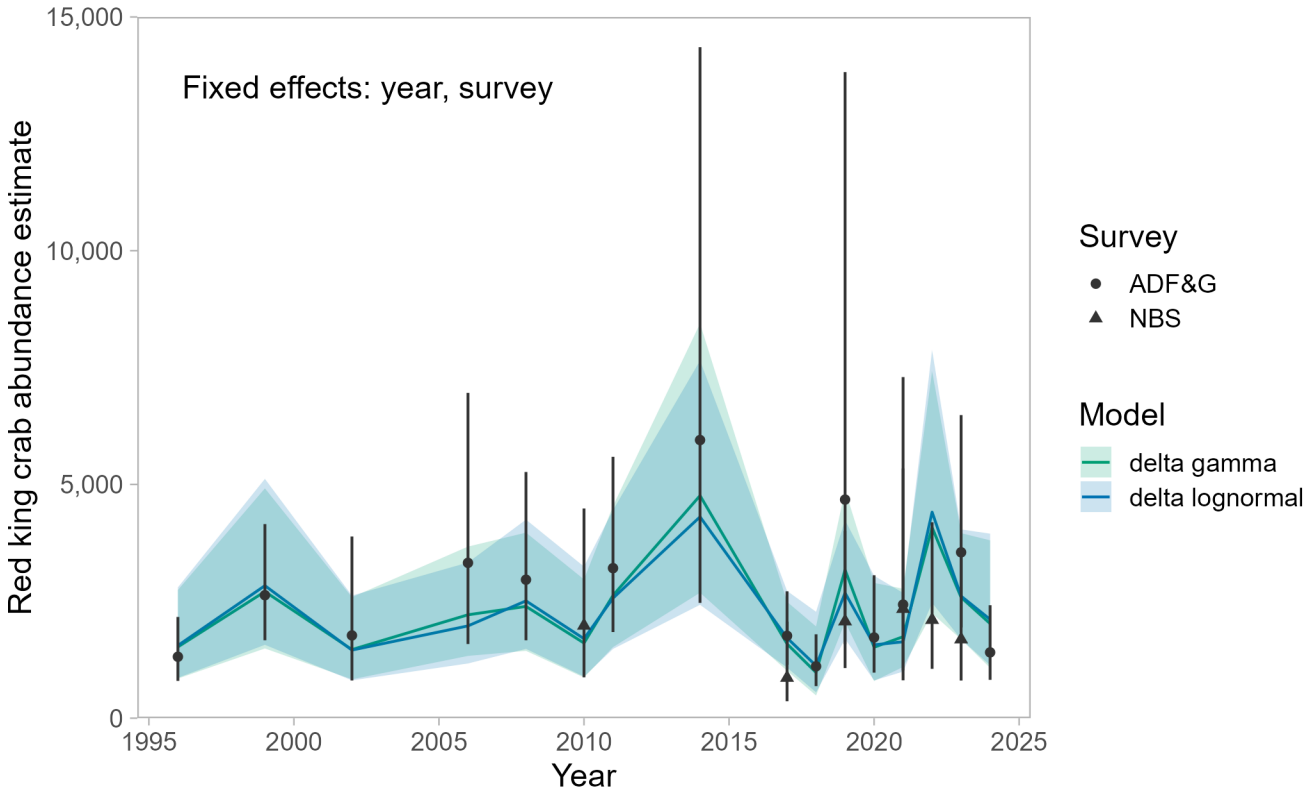


Figure 36: Estimated abundance (1000's of crab) using the smaller prediction grid for male Norton Sound red king crab with carapace length $\geq$ 64 mm from models combining data from the ADF&G and NBS trawl surveys. Colored lines represent abundance ($\pm$95% CI) estimated using sdmTMB with either the delta gamma (green) or delta lognormal (blue) distribution. Year and survey identity were included as fixed effects. Black points represent design-based abundance ($\pm$95% CI) estimates currently used in the stock assessment model.

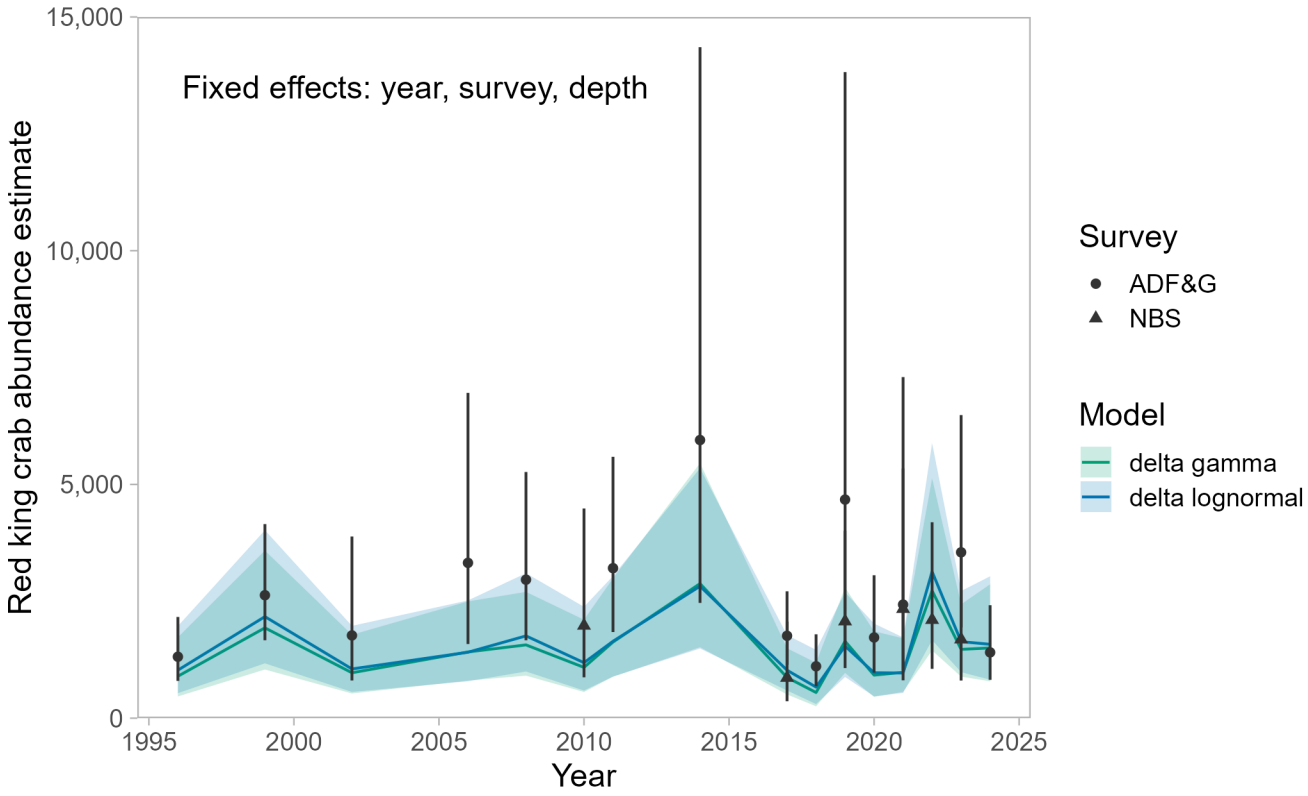


Figure 37: Estimated abundance (1000's of crab) using the smaller prediction grid for male Norton Sound red king crab with carapace length $\geq$ 64 mm from models combining data from the ADF&G and NBS trawl surveys. Colored lines represent abundance ($\pm$95% CI) estimated using sdmTMB with either the delta gamma (green) or delta lognormal (blue) distribution. Year, survey identity, and depth were included as fixed effects. Black points represent design-based abundance ($\pm$95% CI) estimates currently used in the stock assessment model.

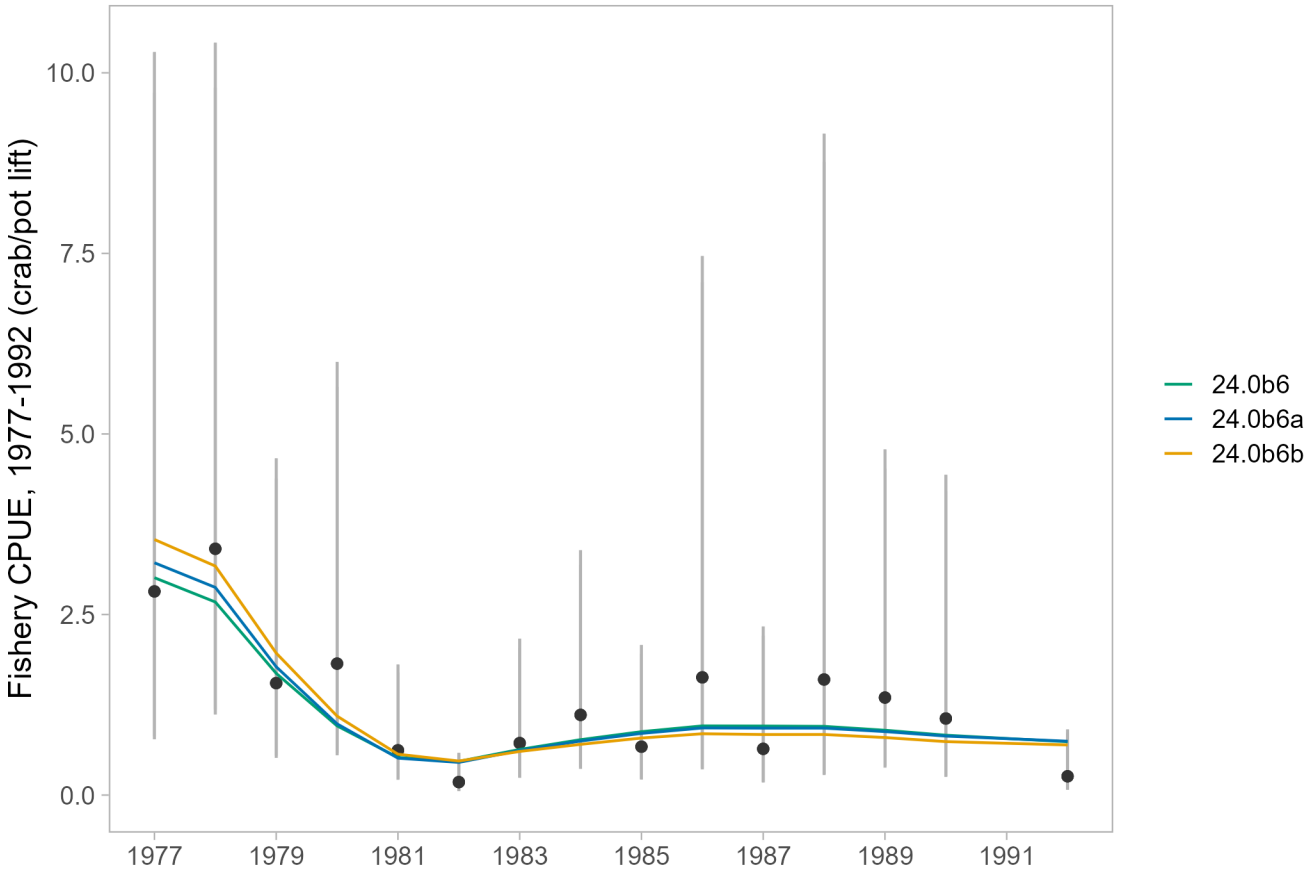


Figure 38: Model fits to the summer commercial fishery standardized CPUE index (1977-1992) for model 24.0b6, the stock assessment model using design-based indices for each of the three trawl surveys (NOAA Norton Sound, NOAA NBS, and ADF&G); model 24.0b6a, the stock assessment model using a design-based index for the NOAA Norton Sound trawl survey and a spatiotemporal model-based index combining data from the NOAA NBS and ADF&G trawl surveys; and model 24.0b6b, the stock assessment model using a spatiotemporal model-based index combining data from the NOAA NBS and ADF&G trawl surveys (no design-based survey indices).

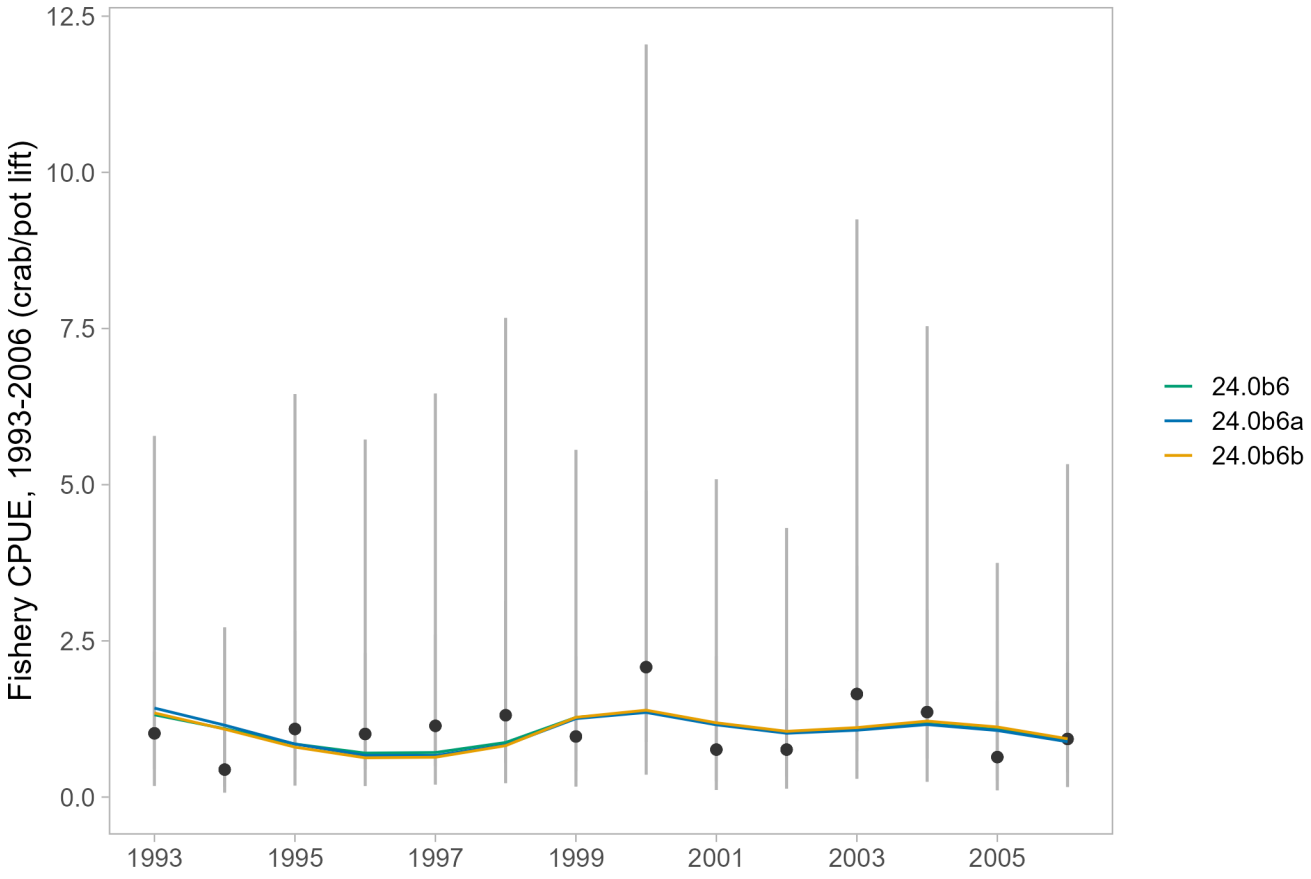


Figure 39: Model fits to the summer commercial fishery standardized CPUE index (1993-2006) for model 24.0b6, the stock assessment model using design-based indices for each of the three trawl surveys (NOAA Norton Sound, NOAA NBS, and ADF&G); model 24.0b6a, the stock assessment model using a design-based index for the NOAA Norton Sound trawl survey and a spatiotemporal model-based index combining data from the NOAA NBS and ADF&G trawl surveys; and model 24.0b6b, the stock assessment model using a spatiotemporal model-based index combining data from the NOAA NBS and ADF&G trawl surveys (no design-based survey indices).

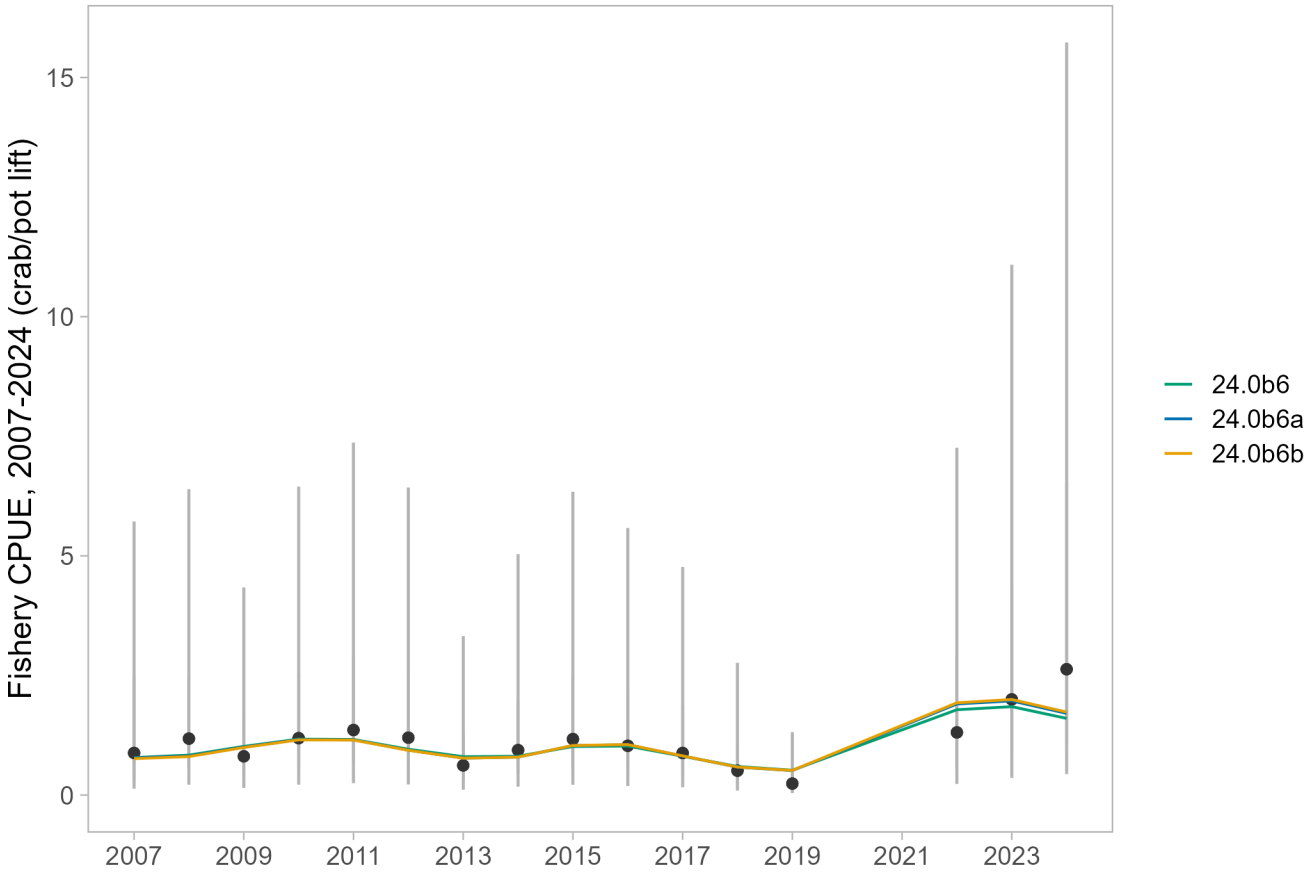


Figure 40: Model fits to the summer commercial fishery standardized CPUE index (2007-2024) for model 24.0b6, the stock assessment model using design-based indices for each of the three trawl surveys (NOAA Norton Sound, NOAA NBS, and ADF&G); model 24.0b6a, the stock assessment model using a design-based index for the NOAA Norton Sound trawl survey and a spatiotemporal model-based index combining data from the NOAA NBS and ADF&G trawl surveys; and model 24.0b6b, the stock assessment model using a spatiotemporal model-based index combining data from the NOAA NBS and ADF&G trawl surveys (no design-based survey indices).

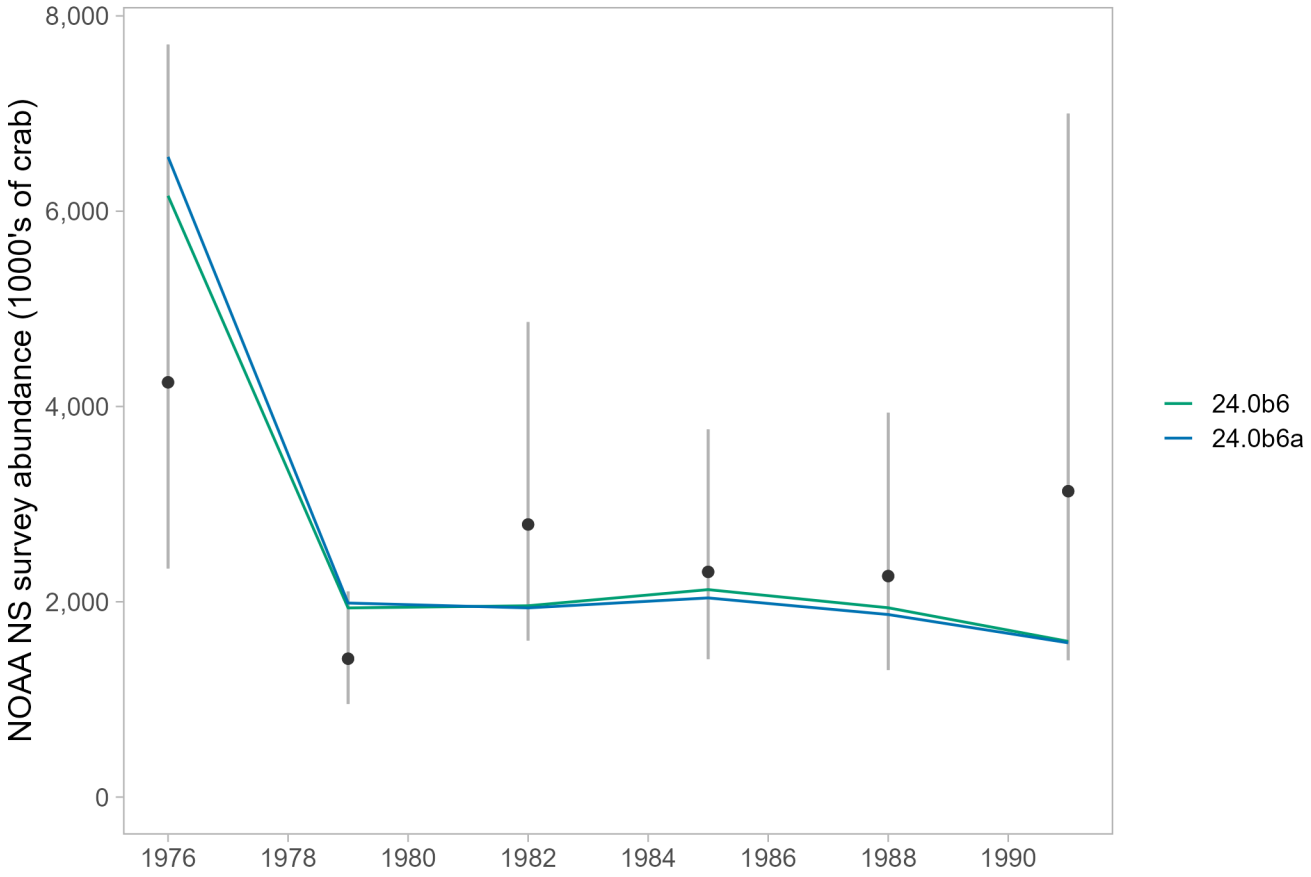


Figure 41: Model fit to the design-based index of abundance from the NOAA Norton Sound trawl survey for model 24.0b6, the stock assessment model using design-based indices for each of the three trawl surveys (NOAA Norton Sound, NOAA NBS, and ADF&G), and model 24.0b6a, the stock assessment model using a design-based index for the NOAA Norton Sound trawl survey and a spatiotemporal model-based index combining data from the NOAA NBS and ADF&G trawl surveys.

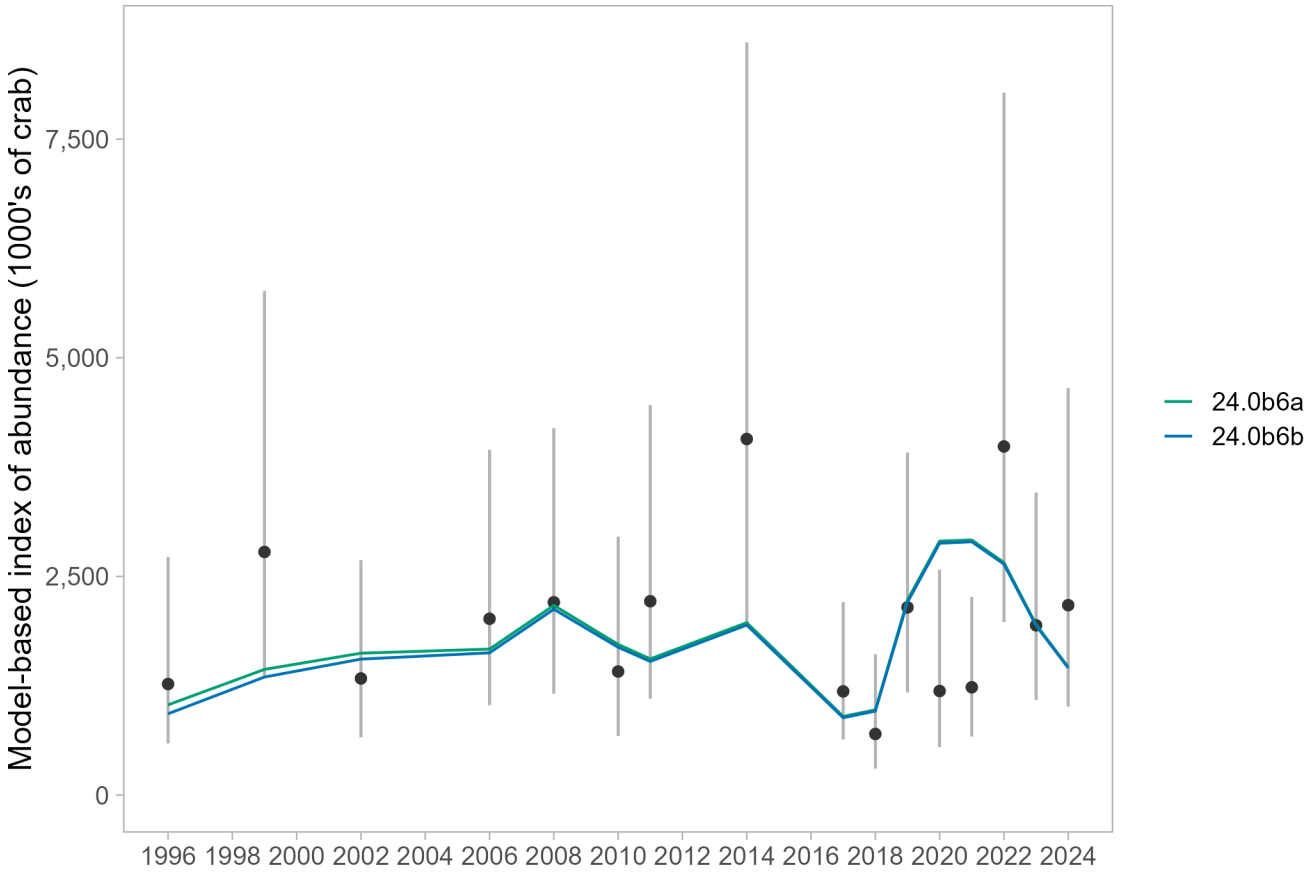


Figure 42: Model fit to the model-based index of abundance for model 24.0b6a, the stock assessment model using a design-based index for the NOAA Norton Sound trawl survey and a spatiotemporal model-based index combining data from the NOAA NBS and ADF&G trawl surveys, and model 24.0b6b, the stock assessment model using a spatiotemporal model-based index combining data from the NOAA NBS and ADF&G trawl surveys (no design-based survey indices).

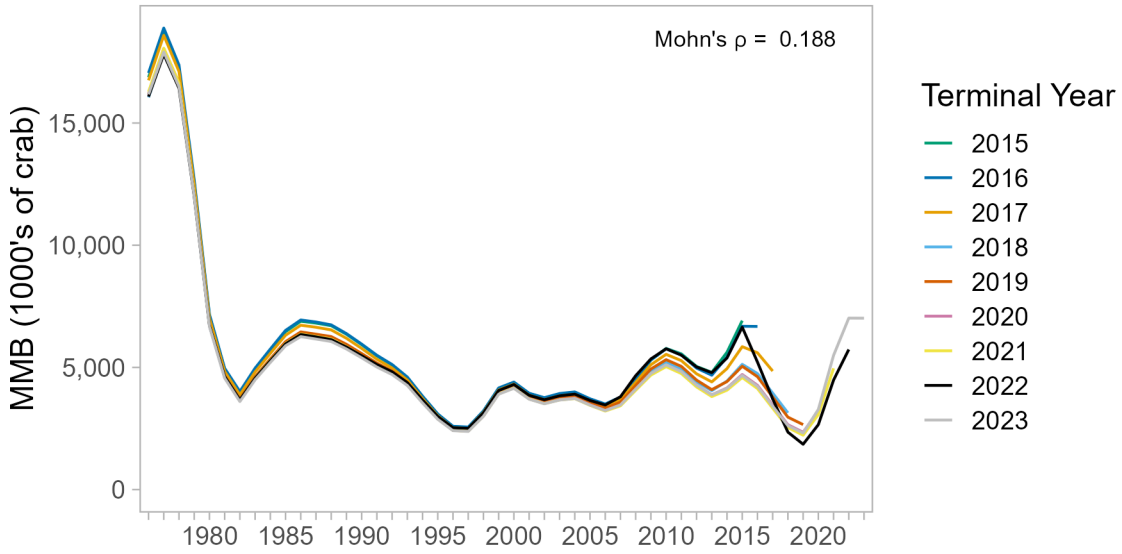


Figure 43: Retrospective patterns in estimated mature male biomass (MMB) for model 24.0b6, the stock assessment model using design-based indices for each of the three trawl surveys (NOAA Norton Sound, NOAA NBS, and ADF&G).

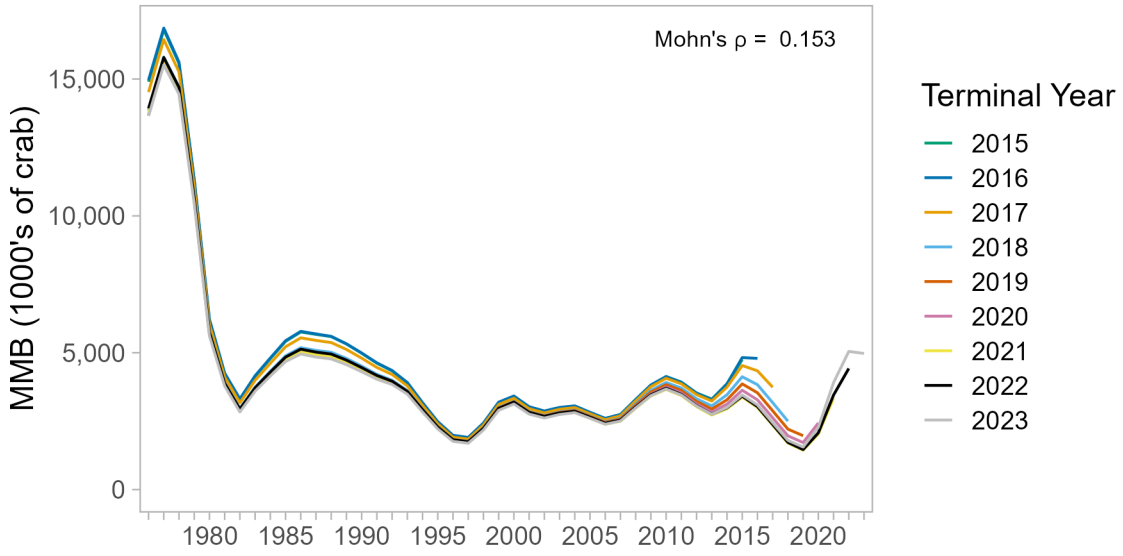


Figure 44: Retrospective patterns in estimated mature male biomass (MMB) for model 24.0b6a, the stock assessment model using a design-based index for the NOAA Norton Sound trawl survey and a spatiotemporal model-based index combining data from the NOAA NBS and ADF&G trawl surveys.

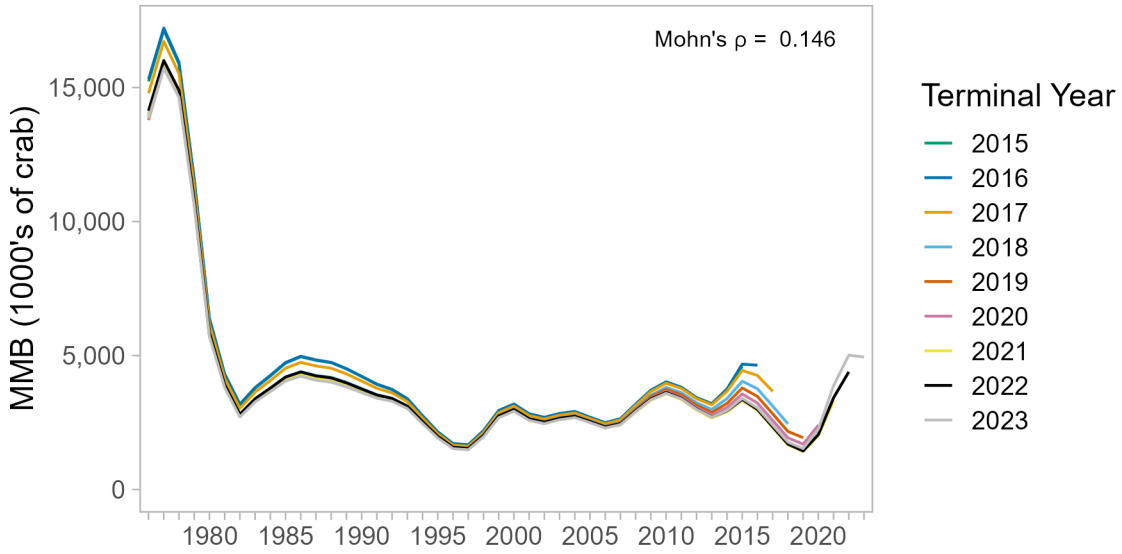


Figure 45: Retrospective patterns in estimated mature male biomass (MMB) for model 24.0b6b, the stock assessment model using a spatiotemporal model-based index combining data from the NOAA NBS and ADF&G trawl surveys, and no design-based survey indices.

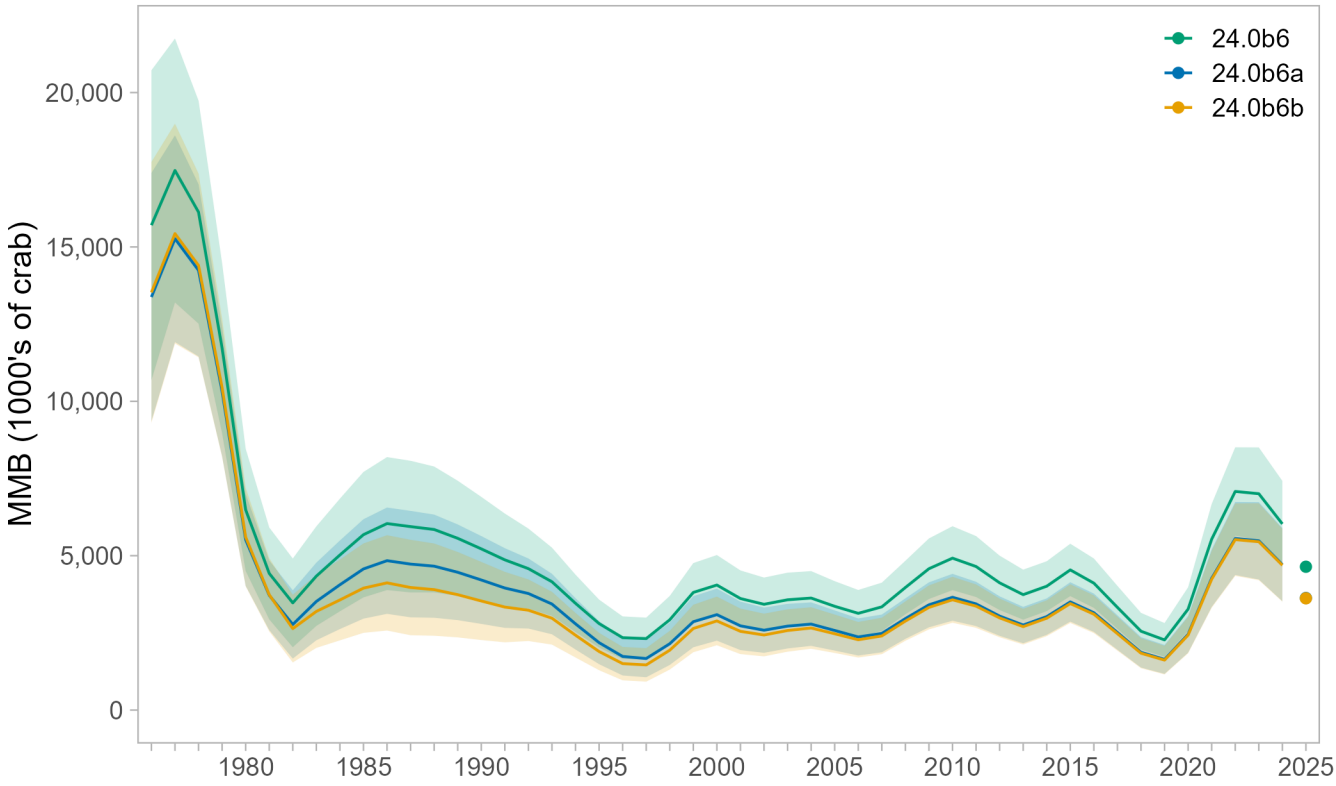


Figure 46: Comparisons of estimated mature male biomass (MMB) time series over 1976-2024 for the stock assessment model using design-based indices for each of the three trawl surveys (24.0b6), the stock assessment model using a design-based index for the NOAA Norton Sound trawl survey and a spatiotemporal model-based index combining data from the NOAA NBS and ADF&G trawl surveys (24.0b6a), and the stock assessment model using a spatiotemporal model-based index combining data from the NOAA NBS and ADF&G trawl surveys (no design-based survey indices; 24.0b6b). Points represent projected values for 2025.